

## Odd–Even Effects in Charge Transport across Self-Assembled Monolayers

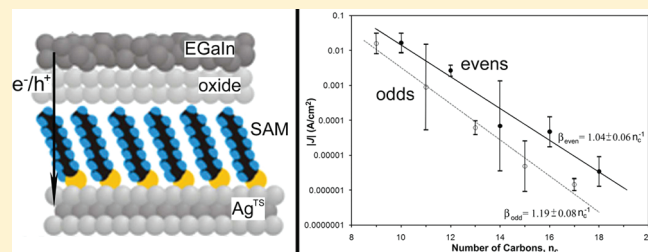
Martin M. Thuo,<sup>†</sup> William F. Reus,<sup>†</sup> Christian A. Nijhuis,<sup>‡</sup> Jabulani R. Barber,<sup>†</sup> Choongik Kim,<sup>†</sup> Michael D. Schulz,<sup>†</sup> and George M. Whitesides<sup>\*†</sup>

<sup>†</sup>Department of Chemistry and Chemical Biology, Harvard University, 12 Oxford Street, Cambridge, Massachusetts 02138, United States

<sup>‡</sup>Department of Chemistry, National University of Singapore, 3 Science Drive 3, Singapore 117543

Supporting Information

**ABSTRACT:** This paper compares charge transport across self-assembled monolayers (SAMs) of *n*-alkanethiols containing odd and even numbers of methylenes. Ultraflat template-stripped silver ( $\text{Ag}^{\text{TS}}$ ) surfaces support the SAMs, while top electrodes of eutectic gallium–indium (EGaIn) contact the SAMs to form metal/SAM//oxide/EGaIn junctions. The EGaIn spontaneously reacts with ambient oxygen to form a thin ( $\sim 1 \text{ nm}$ ) oxide layer. This oxide layer enables EGaIn to maintain a stable, conical shape (convenient for forming microcontacts to SAMs) while retaining the ability to deform and flow upon contacting a hard surface. Conical electrodes of EGaIn conform (at least partially) to SAMs and generate high yields of working junctions.  $\text{Ga}_2\text{O}_3/\text{EGaIn}$  top electrodes enable the collection of statistically significant numbers of data in convenient periods of time. The observed difference in charge transport between *n*-alkanethiols with odd and even numbers of methylenes — the “odd–even effect” — is statistically discernible using these junctions and demonstrates that this technique is sensitive to small differences in the structure and properties of the SAM. Alkanethiols with an even number of methylenes exhibit the expected exponential decrease in current density,  $J$ , with increasing chain length, as do alkanethiols with an odd number of methylenes. This trend disappears, however, when the two data sets are analyzed together: alkanethiols with an even number of methylenes typically show higher  $J$  than homologous alkanethiols with an odd number of methylenes. The precision of the present measurements and the statistical power of the present analysis are only sufficient to identify, with statistical confidence, the difference between an odd and even number of methylenes with respect to  $J$ , but not with respect to the tunneling decay constant,  $\beta$ , or the pre-exponential factor,  $J_0$ . This paper includes a discussion of the possible origins of the odd–even effect but does not endorse a single explanation.



### INTRODUCTION

This paper describes charge transport through tunneling junctions of self-assembled monolayers (SAMs) of *n*-alkanethiols, formed on ultraflat Ag electrodes, contacted with a liquid top electrode. It compares charge transport through SAMs of *n*-alkanethiols having odd and even numbers of methylene groups ( $\text{SC}_{n-1}\text{CH}_3$ , where  $n = 9–18$ ) and demonstrates, using statistical analysis, the existence of an “odd–even effect”. This work constitutes a benchmark both for the theory of charge tunneling in thin organic films and for future experimental work with these systems.

We used EGaIn (a liquid eutectic alloy, 75.5 wt % Ga and 24.5 wt % In) as a liquid-metal top electrode and measured current density,  $J$  ( $\text{A}/\text{cm}^2$ ), through SAMs as a function of applied bias,  $V$  (V). Under ambient conditions, EGaIn has a thin ( $\sim 1 \text{ nm}$ ) surface layer composed predominantly of gallium(III) oxide ( $\text{Ga}_2\text{O}_3$ ).<sup>1</sup> This composite structure — bulk liquid metal supporting a thin rigid, superficial oxide — constitutes a semiconformal (i.e., conformal on length scales exceeding  $1 \mu\text{m}$ , but probably not conformal on the nanoscale) electrode. Together with ultraflat,

template-stripped Ag substrates and alkanethiol SAMs, this top electrode is a crucial component of a system that makes it practical to generate large numbers of  $J(V)$  data ( $\sim 500$  measurements in one day) and gives high yields ( $\sim 80\%$ ) of nonshorting junctions; this combination enables meaningful statistical analysis and opens the door to systematic physical–organic studies of charge transport across organic thin films.

Across the range of molecular lengths,  $d$ , examined, we found that, for a given applied voltage,  $J$  roughly obeys a simple approximation of the Simmons equation,

$$J = J_0 e^{-\beta d} \quad (1)$$

where  $\beta (n_C^{-1})$  is the tunneling decay constant,  $d$  (in  $n_C$ ) is the thickness of the SAM, and  $J_0$  is the current density across a hypothetical SAM lacking an alkyl chain (i.e.,  $d = 0$ ). The magnitude of  $J_0$  is determined by the interfaces between the electrodes and the SAM.

Received: October 7, 2010

Published: February 16, 2011

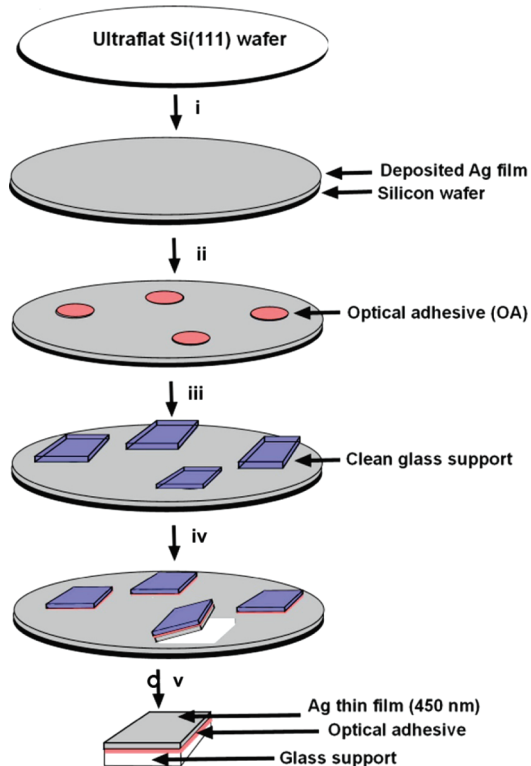


**Figure 1.** Schematic description of the preparation of the template-stripped silver,  $\text{Ag}^{\text{TS}}$ , substrates. (i) On a clean Si(111) wafer, having a native  $\text{SiO}_2$  surface layer, we deposited a 450 nm thick Ag film by e-beam evaporation. (ii,iii). Glass supports were mounted on the thin film using photocurable optical adhesive. A variety of sizes can be used as support, and there is no need for size specification. (iv) After photocuring of the optical adhesive, the metal film around the glass support was cut out using a razor blade. (v) The silver film, with its supporting glass, was lifted off to expose an ultraflat Ag film. The detached  $\text{Ag}^{\text{TS}}$  surface was then immediately ( $\sim 30$  s) used to prepare SAMs by transferring (through air) into a solution of alkanethiol. The Supporting Information gives more details on this procedure.

SAMs of odd-numbered *n*-alkanethiols differ from corresponding SAMs of even-numbered *n*-alkanethiols with respect to many properties, including structure, surface free energy, kinetics of molecular exchange, tribology, kinetics of electron transfer, electrochemistry, reactivity, and packing density.<sup>2–4</sup> In addition to SAMs, liquid crystals and molecule-capped quantum dots also exhibit odd–even effects.<sup>2,5–38</sup> With respect to charge transport in organic systems, the effects of odd- or even-numbered *n*-alkyl or oligomethylene groups have been observed in pentacene-based field-effect transistors,<sup>39</sup> H-bonded assemblies,<sup>40</sup> and biphenyl-based systems.<sup>41</sup> Thus, it is not astonishing, although still noteworthy, that odd–even effects also influence charge transport across SAMs of alkanethiols.<sup>2,34–38,42,43</sup>

We synthesized a series of *n*-alkanethiols with an odd number of carbons ( $\text{SC}_n$ , where  $n = 9, 13, 17$ ). Commercially available undecanethiol, pentadecanethiol, and all even-number methylene-containing thiols were purified before use (see Supporting Information). We formed SAMs on template-stripped silver (abbreviated  $\text{Ag}^{\text{TS}}$ ) (Figure 1). We then fabricated molecular tunneling junctions by bringing the SAMs into contact with a  $\text{Ga}_2\text{O}_3/\text{EGaIn}$  liquid top electrode. [We use this nomenclature to emphasize the importance of the surface film of Ga(III) oxide,

but note that this description is a simplification of a more complex surface.<sup>44</sup>]

Using statistical tools, we showed, with >95% confidence, that the results from SAMs with even and odd numbers of methylenes belong to separate data sets (i.e., analyzing the two series separately led to more consistent interpretations of the results, according to the simplified Simon's model, than did analyzing them together); thus, we concluded that there is an odd–even effect. While the data from SAMs with even and odd numbers of methylenes demanded separate fits to eq 1, our statistical analysis was not sufficiently powerful to distinguish between the values of  $J_0$  and  $\beta$  for these two series.

Four characteristics of these junctions enabled us to perform physical–organic experiments relating molecular structure to charge transport: (i) a semiconformal top electrode, (ii) ultraflat (root-mean-square roughness <0.5 nm as measured by atomic force microscopy) template-stripped silver substrates, (iii) carefully purified thiols, and (iv) the ability to conduct measurements under ambient conditions (i.e., without a clean room, a polymer interface, or a solvent bath). The first three characteristics of these junctions reduced the density of defects leading to shorts and outliers (defined below) and increased the yield of working junctions. The fourth characteristic allowed the collection of large numbers of data within a convenient time frame ( $\sim 500$   $J(V)$  traces in a day) and, thus, enabled robust statistical analysis.

Charge transport through insulating organic matter almost certainly occurs (at least over distances of less than a few nanometers) via nonresonant coherent tunneling.<sup>39,45–55</sup> Understanding the relationship between molecular structure and electronic properties in organic systems would improve our ability (i) to model electron transport in relevant biological systems (e.g., redox proteins) and (ii) to evaluate the potential of, and perhaps to design, electronic devices based on organic components. To these ends, we wished to develop a convenient and reliable technique for conducting physical–organic experiments designed to probe the fundamental principles of charge transport across thin (<3 nm) films of structurally well-defined organic matter.

Systematic studies of charge transport in small molecules have been experimentally difficult, and there is currently no convenient, broadly accepted platform with which to perform such studies. Probing the difference between SAMs of *n*-alkanethiols with odd and even numbers of methylene units is an example of a systematic, physical–organic study designed to give information about the effect of the noncovalent interface (see below) between the SAM and an electrode on charge transport.

We and others<sup>50,56–67</sup> have begun an effort to develop and prove reliable protocols for measuring charge transport across SAMs. Our approach features a semiconformal (mechanically compliant on the micrometer scale but probably not conformal on smaller scales) liquid top electrode, EGaIn (a liquid eutectic alloy of gallium and indium), whose surface is largely or entirely covered with a thin oxide film (predominantly gallium oxide).<sup>44</sup> We believe that this oxide film is crucial to generating high yields of working junctions (see below) and, thus, enables the collection and statistical analysis of large numbers of data.

There are, however, several features of the layer of  $\text{Ga}_2\text{O}_3$  that merit careful consideration and discussion. The electrical resistivity ( $\sim 10^6 \Omega\text{-cm}$ )<sup>1</sup> of this oxide layer is at least 3 orders of magnitude smaller than that of a SAM of  $\text{SC}_9$  (the shortest SAM we are able to measure reliably). Since the thickness of this layer ( $\sim 1$  nm) is approximately equal to that of a typical SAM, the resistance of this layer is several orders of magnitude

less than that of a SAM. The roughness of the layer of  $\text{Ga}_2\text{O}_3$  probably causes the electrode to be nonconformal over distances up to 1  $\mu\text{m}$ , a characteristic that adds uncertainty to the estimation of the area of junctions. On the basis of experiments and simulations that will be discussed elsewhere,<sup>1</sup> however, we believe that overestimation of junction area introduces a systematic error, as opposed to a random error. In other words, distributions of  $J$  may be shifted, but not broadened, by this error. Furthermore, we have no reason to suspect that this error varies with the length of the SAM; therefore, it should not affect comparisons across alkanethiols of different lengths. Finally, the surface of the  $\text{Ga}_2\text{O}_3$  may be contaminated with a complete or partial layer of adsorbed organics. The effect of this layer on charge transport is unknown. We show in this work that, despite these cautionary features, the  $\text{Ga}_2\text{O}_3/\text{EGaIn}$  electrode yields results that are reproducible and consistent with a wide range of prior work on charge transport through SAMs of *n*-alkanethiols. Further, the distributions observed for compounds at the extremes of the series ( $\text{SC}_9$  and  $\text{SC}_{10}$  on the lower end and  $\text{SC}_{16}$ – $\text{SC}_{18}$  on the upper end) were consistently narrower than those of compounds in the middle of the series ( $\text{SC}_{11}$ – $\text{SC}_{15}$ , with the exception of  $\text{SC}_{13}$ , see below). We infer that the nature of the interfaces in the junctions does not dominate the broad distributions observed in the middle of the series.

## ■ BACKGROUND

Some common features have emerged in many of the systems for studying charge transport in organic matter. Self-assembled monolayers are an obvious candidate for the organic component of such systems, since SAMs are readily prepared using organic precursors having a wide range of structures. Gold and silver are currently the most widely used metal substrates for forming SAMs. Gold has the advantage of being impervious to oxidation under ambient conditions; however, the alkyl chains of SAMs of alkanethiols on gold are tilted at an angle of  $\sim 30^\circ$  to the surface normal, compared to  $\sim 10^\circ$  on Ag.<sup>68–71</sup> Outka et al.<sup>72</sup> and Ulman et al.<sup>73</sup> illustrated that an optimal packing density of *n*-alkanethiols on a metal surface depends on a combination of the tilt angle and lattice spacing. Subsequently, it has been shown that thiolate SAMs on Ag(111) have 26% more chains per unit area than on Au(111).<sup>74,75</sup> While most studies use substrates (whether Au or Ag) as-deposited by electron-beam evaporation, we have previously shown that template-stripping leads to flatter surfaces (rms roughness;  $\text{Ag}^{\text{TS}} = 1.2$  vs 5.1 for as-deposited, and  $\text{Au}^{\text{TS}} = 0.6$  vs 4.5 for as-deposited)<sup>76</sup> and increases the yield of nonshorting junctions when using a Hg top electrode.<sup>76,77</sup>

While there is a broad consensus on the use of SAMs and, to a large extent, Au or Ag substrates, myriad strategies exist for forming a second (top) contact to the SAM. Historically, forming an electrical contact with a SAM has been challenging. Lee et al. have shown that direct evaporation of metallic top electrodes onto SAMs damages the monolayer<sup>56,59,78,79</sup> and results in low yields (<5%) of nonshorting junctions and in the formation of metal filaments due to the migration of metal atoms through defect sites in the SAM. With the notable exception of the work of Lee et al.,<sup>56,59,60</sup> who reported yields and statistically defined “working devices” for these junctions, studies of evaporated metal top electrodes have not included adequate statistical analysis of  $J(V)$  data and are, thus, unable to discriminate between molecular effects and artifacts. When performed carefully, these studies can afford reproducible results, but only when

sufficiently large numbers of electrodes are generated to define the system statistically. These types of preparations and measurements are too arduous for physical–organic studies. Furthermore, many of these studies use SAMs formed from structurally complex molecules, without adequate characterization of the probably complex and often disordered structure of these SAMs.

Other strategies for measuring charge transport across SAMs fall into two arbitrary categories: (i) small-area ( $<1 \mu\text{m}^2$ , or  $1\text{--}10^6$  molecules) measurements, which can generate high-quality data but are time-consuming to perform and require specialized techniques and instruments, and (ii) large-area ( $>100 \mu\text{m}^2$ , or  $10^8\text{--}10^{12}$  molecules) measurements aimed at conveniently generating sufficiently large numbers of data to allow statistical assessment of experimental uncertainty. In the first category, Lindsay and co-workers,<sup>50,80–82</sup> Frisbie and co-workers,<sup>83–88</sup> Lee and co-workers,<sup>56,58,89–91</sup> Venkataraman and co-workers,<sup>92–94</sup> and others<sup>95</sup> have employed conducting probe tips (STM, cpAFM) to measure charge transport across SAMs. Break junctions, both mechanically controllable and electromigration-based, are another form of small-area junctions (consisting of one to several molecules trapped between two electrodes<sup>60,96–99</sup>). Break junctions have the distinct advantage of incorporating a gate electrode, although they are tedious to prepare. Kushmerick et al. developed a technique for measuring small-area molecular junctions ( $\sim 10^3$  molecules) through a crossed-wire tunneling junction.<sup>100,101</sup> Two gold wires ( $10 \mu\text{m}$  diameter) are crossed, with one parallel and the other perpendicular to an external magnetic field. A current flowing through the perpendicular wire engenders a Lorenz force that controls the spacing between the two wires. In this technique, one wire — coated with a  $\pi$ -conjugated self-assembled monolayer — creates a metal–molecule–metal junction.<sup>102</sup>

For large-area measurements of SAMs on Ag, we and others have employed a hanging drop of Hg, on which a second SAM has been formed.<sup>53,77,103–110</sup> Recently, Akkerman et al. fabricated large numbers of molecular junctions in parallel using a spin-cast, conductive polymer film (PEDOT:PSS) on top of the SAM to make electrical contacts and to protect the organic molecules from damage due to exposure of evaporated metal atoms.<sup>62–66</sup> The conductive polymer film may be protective and provide a good contact; unfortunately, it also introduces unresolved ambiguities in the system and seems to produce measurements that are rather different from those obtained with other methods ( $\beta_{\text{even}} = 0.66 \pm 0.04$  per carbon, where the consensus value from other methods is  $\beta_{\text{even}} \approx 1$  per carbon,  $n_C^{-1}$ , for *n*-alkanethiol SAMs).<sup>63</sup>

Although a wide range of methods have been employed to measure charge transport across SAMs, nearly all *successful* techniques share the characteristic that they have a nonmetallic layer between the SAM and the top electrode: a thin film of insulating metal oxide, a small gap of air or vacuum between a probe tip and the SAM, a second SAM on Hg, or a layer of conductive polymer between the SAM and an evaporated Au electrode. The only exception to this rule appears to be the use of cpAFM techniques, in which a bare metal electrode, under a controlled load of force, directly contacts the SAM; all successful large-area ( $>100 \mu\text{m}^2$ ) junctions, however, incorporate a protective layer. The most probable function of this “protective layer” in these junctions is to prevent metal atoms from migrating through defect sites under electrostatic pressure and causing filaments to form and thus to cause shorts and other artifacts. In our current

work, a  $\sim 2$  nm thick self-passivating semiconducting oxide ( $\text{Ga}_2\text{O}_3$ ) layer performs this function.<sup>1</sup>

The best characterized types of SAMs, both structurally and with respect to charge transport, are those formed by *n*-alkanethiols on Au and Ag.<sup>3,52,69,99,111–131</sup> The mechanism of charge transport through SAMs is believed to be hole tunneling, with the height of the tunneling barrier defined by the large HOMO–LUMO gap (8–10 eV) of the alkanethiols forming the SAM.<sup>132</sup> The barrier width is defined by the thickness of the SAM ( $\sim 1$ – $3$  nm). The value of the tunneling decay constant,  $\beta$  (eq 1), reported in the literature for the commercially available even-numbered alkanethiols ( $\text{CH}_3(\text{CH}_2)_{n-1}\text{SH}$ , where  $n = 10, 12, 14, 16, 18$ ) ranges from 0.51 to  $1.13 \text{ n}_\text{C}^{-1}$ , with a majority of the values in the range  $0.75$ – $1.1 \text{ n}_\text{C}^{-1}$ .<sup>59,63,65,133</sup> Akkerman and others<sup>39,53,132,134</sup> attempted to distinguish charge transport across SAMs comprising odd and even numbers of methylenes experimentally but did not succeed.

SAMs of *n*-alkanethiols assembled on metal surfaces via a covalent interaction pack with a distinct tilt that is characteristic of the substrate (e.g.,  $\sim 10^\circ$  for Ag,  $\sim 30^\circ$  for Au, with respect to the surface normal). The hybridization, and hence both the geometry and stereoelectronic environment, around the sulfur atom is also believed to depend on the substrate ( $\text{sp}^3$  for Au and  $\text{sp}$  for Ag).<sup>3,69,135</sup> For *n*-alkanethiols in an all-*trans* extended conformation, three parameters combine to determine the orientation of the terminal group at the surface of the SAM: (i) the tilt angle, (ii) the hybridization around the sulfur atom, and (iii) the number of methylenes in the alkyl chain. The orientation of the terminal methyl group, in turn, affects the surface properties of the SAM and therefore dictates the nature of interactions with other materials.

In reality, SAMs are not extended, perfect, 2D crystals but have many defects: pinholes, domain boundaries, disordered regions, impurities physisorbed on or incorporated into the SAM, and defects due to vacancy islands, step edges, and grain boundaries in the substrate, to name a few.<sup>3,69,77,136</sup> These defects cause many of the molecules in a SAM to adopt conformations other than the ideal all-*trans* extended conformation. Defects in the SAMs may thus blur the distinction between the surfaces presented by odd- and even-numbered alkanethiols — a distinction that would probably manifest itself most significantly in the difference in the orientations of their terminal methyl groups in the *trans*-extended conformation. The more disordered the SAM, the less important we expect intrinsic, conformational-based differences between odd- and even-numbered *n*-alkanethiols to be.

Liquid top electrodes (e.g., Hg, Hg-SR, and  $\text{Ga}_2\text{O}_3/\text{EGaIn}$ ) form reproducible contacts with SAMs and can be used to generate large numbers of data, the distributions of which can be analyzed statistically. Although they have their own limitations, liquid top electrodes are easier to use, and require less specialized equipment, than other methods (e.g., STM tip-based techniques or break junctions) and give information averaged over a relatively large area (and thus, in principle, relevant to devices). The AFM-based methods are outstanding for characterizing a range of behaviors at molecular granularity. This paper extends previous work on the  $\text{Ga}_2\text{O}_3/\text{EGaIn}$ -based system of measuring tunneling currents across SAMs on  $\text{Ag}^{\text{TS}}$  and demonstrates an odd–even effect in charge transport across alkanethiol SAMs.

Our initial estimate, using a  $\text{Ga}_2\text{O}_3/\text{EGaIn}$  top electrode, was  $\beta_{\text{even}} \approx 0.54 \text{ n}_\text{C}^{-1}$ .<sup>137</sup> This value lies well outside the band of

values more commonly reported in literature ( $0.75$ – $1.1 \text{ n}_\text{C}^{-1}$ ). We now believe this number to be incorrect and to reflect an inappropriate selection of data from a sparse and (at that time) noisy data set. We measured the value of  $J$  ( $\text{A}/\text{cm}^2$ ) for four chain lengths ( $\text{SC}_{10}$ ,  $\text{SC}_{12}$ ,  $\text{SC}_{14}$ , and  $\text{SC}_{16}$ ) but used only three ( $\text{SC}_{12}$ ,  $\text{SC}_{14}$ , and  $\text{SC}_{16}$ ) in determining the value of  $\beta_{\text{even}}$ . The collected results should, however, have been analyzed without excluding any data. We made three errors: (i) For reasons that seemed valid at the time but, in retrospect, were not, we discarded the data for  $\text{SC}_{10}$ . Had we instead fitted the data derived from all four alkanethiols, we would have estimated  $\beta$  close to  $1.0 \text{ n}_\text{C}^{-1}$  (albeit with a large experimental uncertainty). (ii) In these early stages of development of the  $\text{Ga}_2\text{O}_3/\text{EGaIn}$  electrode, we did not appreciate a number of experimental variables, and the collected data were much more scattered than the data in this paper. The quantity of data, both the number of alkanethiols used and the number of  $J(V)$  traces collected, was insufficient for a reliable statistical analysis. (iii) The purity of the *n*-alkanethiols was not carefully controlled or monitored throughout the study.

In this study, we have corrected these errors by (i) including all data from our analysis (we exclude no data), (ii) collecting more data, both numbers of alkanethiols molecules used (five per series, for a total of ten, as opposed to four in the previous work) and numbers of  $J(V)$  traces measured (an increase of a factor of 3–10 over our previous work<sup>137</sup>), and (iii) purifying all compounds before use. The result is a tunneling decay constant ( $\beta_{\text{even}} = 1.12 \text{ n}_\text{C}^{-1}$ ) for even-numbered alkanethiols that agrees well with the consensus of results based on other liquid metal electrodes.<sup>77,138</sup> In this work, we also obtained  $\beta_{\text{odd}} = 1.03 \text{ n}_\text{C}^{-1}$  for odd-numbered alkanethiols. Although this is numerically different from the value obtained from the even series, the difference between  $\beta_{\text{even}}$  and  $\beta_{\text{odd}}$  is not statistically significant, according to a two-tailed Student's *t* test ( $p > 0.1$ ). The lack of a statistically significant difference is not, however, a statement that the values of  $\beta_{\text{odd}}$  and  $\beta_{\text{even}}$  are the same, and this apparent difference suggests a direction for further investigation. Fitting the two series yields values of  $J_0$  with overlapping ranges of uncertainty.

## ■ EXPERIMENTAL DESIGN

**Template-Stripped Ag Substrates.** We used a silver surface because the SAMs have a smaller tilt angle ( $\sim 10^\circ$  to the surface normal), which leads to better packing (SAMs on  $\text{Ag}(111)$  surfaces have  $\sim 26\%$  more alkyl chains/unit area than do those on  $\text{Au}(111)$ ).<sup>74,75</sup> We use template-striped silver ( $\text{Ag}^{\text{TS}}$ ) substrates because the surface is flatter, and probably cleaner, than the exposed, top surface of electron-beam evaporated films ( $\text{Ag}^{\text{AD}}$ ).<sup>76</sup> We previously found that the use of template-striped substrates rather than as-deposited substrates significantly increased the yield of working junctions in SAM-based devices.<sup>76,77</sup>

**Liquid-Metal Top Electrode.** EGaIn is commercially available in high purity, easy to handle, and nontoxic. On exposure to ambient conditions, EGaIn forms a thin ( $\sim 2$  nm), self-limiting passivating gallium(III) oxide film on the surface.<sup>44,139</sup> The remarkable mechanical strength of this film is responsible for the ability of EGaIn to adopt and maintain nonequilibrium shapes (e.g., the cone used to make electrical contacts in this paper).<sup>137</sup>

**Self-Assembled Monolayers.** Self-assembled monolayers of *n*-alkanethiols on silver give well-defined organic structures. These SAMs provide an obvious substrate for studying charge transport because they (i) are constrained in one dimension to the length of the molecule ( $\sim 2$  nm), yet (ii) can be arbitrarily large in the other two dimensions,

and (iii) can be readily modified, via simple organic reactions, to increase the complexity of the molecules being investigated.

**Choice of *n*-Alkanethiols.** We used compounds of intermediate chain lengths,  $9 \leq n \leq 18$ . This range avoided problems associated with long chains (low solubility in polar solvents and current densities too low to be measured with our electrometer) and the empirical difficulties (e.g., shorts and noisy, unstable junctions) associated with short chains. The range of alkanethiols used ( $\text{SC}_9\text{--SC}_{18}$ ) are  $\sim 1.0\text{--}2.5$  nm long. This choice of chain lengths also allowed comparison with information in the literature, because SAMs of alkanethiols in this range of chain lengths have been widely studied by others.

**Purity of Thiols.** We emphasize the importance of using highly pure (>99%) alkanethiols. As previously observed by us and others, impurities in the thiols can lead to defects in the SAM and, therefore, to artifacts and decreased yields of working junctions.

**Log-Normal Distributions of  $J$ .** As noted in the Results and Discussion section, we observed log-normal distributions of  $J$  (i.e.,  $\log(|J|)/[\text{A}/\text{cm}^2]$ , written as  $\log(|J|)$  for convenience, was normally distributed). Log-normal distributions of current have been observed previously in molecular junctions by us (using Hg-drop junctions)<sup>77</sup> and others (using polymer buffer layers,<sup>63,67,134</sup> nanopores,<sup>60,140</sup> and cpAFM<sup>87,141,142</sup>). In all of these studies, the explanation for the apparent normal distribution of  $\log(|J|)$  is that  $J$  depends exponentially on a physical parameter that is normally distributed, such as the thickness of the tunneling barrier between two electrodes. This dependence on thickness, across all the above techniques, leads to a range of  $J$  that spans several (3–8) orders of magnitude. We believe that defects in the  $\text{Ag}^{\text{TS}}$  substrate, the SAM, and the  $\text{Ga}_2\text{O}_3/\text{EGaIn}$  top electrode lead to variations in the local separation between electrodes,  $d$  (eq 1). These variations are presumably normally distributed and thus give rise to log-normal distributions of  $J$  (appearing as Gaussian peaks in histograms of  $\log(|J|)$ ).

**Analyzing Distributions of  $\log(|J|)$  vs  $J$ .** Since many of the tools of statistical analysis assume that the data being analyzed are normally distributed, directly analyzing distributions of  $J$  is difficult. A more statistically tractable approach than directly handling  $J$  is to work with  $\log(|J|)$  (since distributions of the latter are normal) and subsequently to map the results of the analysis of  $\log(|J|)$  onto the domain of  $J$ . For instance, we wish to determine the population mean,  $\mu_J$ , and standard deviation,  $\sigma_J$ , of  $J$ . Calculating the arithmetic average of  $J$  ( $\langle J \rangle = (\sum_i J_i)/N_J$ , where  $\sum_i J_i$  is the sum of all measured values of  $J$  and  $N_J$  is the number of measured values of  $J$ ) yields an estimate of the population mean,  $\mu_J$ , strongly biased toward high values of  $J$ . Similarly, the straightforward calculation of the arithmetic standard deviation of  $J$  ( $s = [\langle (J - \langle J \rangle)^2 \rangle]^{1/2}$ ) also yields a biased value. On the other hand, since  $\log(|J|)$  is normally distributed, familiar methods can be used to estimate the population mean,  $\mu_{\log}$ , and standard deviation,  $\sigma_{\log}$ , of  $\log(|J|)$  ( $\mu_J$  is related to  $\mu_{\log}$  by the equation  $\log(\mu_J) = \mu_{\log}$ , and  $\sigma_J$  to  $\sigma_{\log}$  by  $\log(\sigma_J) = \sigma_{\log}$ ). Reporting error is also easier for  $\log(|J|)$  than for  $J$ . For instance, we can correctly report the error on an estimate of the population mean of  $\log(|J|)$  as  $\mu_{\log} \pm \sigma_{\log}$ . The expression  $\mu_J \pm \sigma_J$  does not make sense as a description of the error in the estimate of the population mean of  $J$ , if the distribution of  $J$  is normal in  $\log(|J|)$ .

## ■ RESULTS AND DISCUSSION

**Synthesis and Purification of *n*-Alkanethiols.** We synthesized the  $\text{SC}_9$ ,  $\text{SC}_{13}$ ,  $\text{SC}_{17}$ , and  $\text{SC}_{19}$  alkanethiols from their corresponding primary alkyl bromides. The alkyl bromides were converted to isothiuronium salts, followed by treatment with  $\text{NaOH}$ , which gave the desired thiol. The products, after chromatographic purification, were characterized by NMR, and the spectral data were compared to the literature.

We established and here emphasize the importance of purity of the thiols on the reproducibility of the subsequent electrical

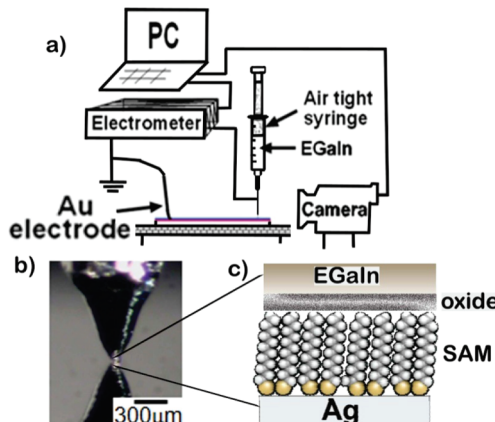


**Figure 2.** (a) Schematic illustration of the apparatus used to make measurements of tunneling currents across SAMs. (b) Picture of a working  $\text{Ag}^{\text{TS}}/\text{SAM}/\text//\text{Ga}_2\text{O}_3/\text{EGaIn}$  junction. The junction was fabricated by gently lowering the EGaIn tip onto a substrate bearing the SAM, and contact was confirmed by the convergence of the tip with its reflected image on the substrate surface to give a closed electrical circuit. The connection was also confirmed by passing current through the closed circuit. (c) Illustration of the anatomy of a perfect junction, showing the van der Waals interface between the SAM and the EGaIn/oxide top electrode.

measurements. We ensured that the alkanethiols had purity of >99% by  $^1\text{H}$  NMR before use. The *n*-alkanethiols degrade over time, especially at elevated temperature and in the presence of oxygen, forming either disulfides or sulfur oxides (see example in the Supporting Information, Figure S5a; 2.67 and 3.73 ppm, respectively). To ensure that our thiols were pure, we either recrystallized them under an inert atmosphere using cannula transfer techniques or purified them by flash column chromatography immediately before storage and, where necessary, before use. The Supporting Information gives a detailed description of our procedures. We found that a single recrystallization often did not give sufficiently pure thiols for our uses, especially when the starting reagents were partially oxidized.

**Preparation and Measurement of Junctions.** We prepared the ultraflat template-stripped surfaces,  $\text{Ag}^{\text{TS}}$ , by depositing 450 nm of Ag metal onto a clean Si(111) wafer using an electron-beam evaporator and then detaching (stripping) the Ag film from the Si wafer using a glass support as previously described and illustrated in Figure 1.<sup>136</sup> SAMs were generated by immersing the  $\text{Ag}^{\text{TS}}$  in a degassed solution of a thiol for 3 h (see Supporting Information for detailed procedures). The  $\text{Ag}^{\text{TS}}/\text{SAM}/\text//\text{Ga}_2\text{O}_3/\text{EGaIn}$  junctions were fabricated as previously discussed.<sup>136,137</sup> The reflection of the tip image on the silver surface was used to confirm a contact between a SAM and the EGaIn top electrode during junction fabrication (Figure 2b).

We collected 380–2800  $J(V)$  data points for every *n*-alkanethiol (synthesized or commercially available) using  $\text{Ag}^{\text{TS}}/\text{SC}_n\text{SAM}/\text//\text{Ga}_2\text{O}_3/\text{EGaIn}$  junctions. For each alkanethiol synthesized, a minimum of 11 junctions ( $\text{Ag}^{\text{TS}}/\text{SC}_n/\text//\text{Ga}_2\text{O}_3/\text{EGaIn}$ ) were fabricated, with a maximum of 11 junctions fabricated per  $\text{Ag}^{\text{TS}}$  chip (a  $\text{Ag}^{\text{TS}}$  surface on a glass substrate). Except in the case of  $\text{SC}_9$ , we measured a minimum of two  $\text{Ag}^{\text{TS}}$  chips per molecule. On each junction, a maximum of 21  $J(V)$  traces (one trace =  $0\text{ V} \rightarrow +0.5\text{ V} \rightarrow -0.5\text{ V} \rightarrow 0\text{ V}$  at steps of 50 mV with a 0.2 s delay; each trace gave two data points each from the forward and reverse sweep) were recorded (Table 1).

**Table 1.** Yield and Other Parameters of Data Collected for Odd- and Even-Numbered Alkanethiols

<i>n</i>	users	samples	junctions	shorting junctions <sup>a</sup>	$N_{ J }$ <sup>b</sup>	nonshorting yield (%) <sup>c</sup>
9	1	1	11	2	376	82
10	4	5	51	6	1836	88
11	4	10	105	13	2844	88
12	4	8	65	8	2428	88
13	2	3	21	1	848	95
14	4	12	101	4	3892	96
15	4	11	81	7	1820	91
16	2	2	21	0	872	100
17	4	5	27	4	742	85
18	3	5	45	1	1306	98

<sup>a</sup> A short is defined in the text as a junction for which  $J$  exceeds  $10^2 \text{ A}/\text{cm}^2$  at any time. <sup>b</sup> The total number of values of  $J$  collected at each applied bias. No data were excluded. <sup>c</sup> Calculated as the ratio of nonshorting junctions to the total number of junctions.

**Attempts To Measure *n*-Alkanethiols Longer than SC<sub>18</sub> and Shorter than SC<sub>9</sub> Failed.** SAMs derived from *n*-alkanethiols longer than SC<sub>18</sub> yielded noisy and inconsistent  $J(V)$  traces similar in shape and magnitude to an open circuit (i.e., a  $J(V)$  trace measured with the Ga<sub>2</sub>O<sub>3</sub>/EGaIn electrode suspended in air). On the basis of a linear fit of our data (see Figure 5, below), we extrapolate a current density for SC<sub>19</sub> of  $8.3 \times 10^{-8} \text{ A}/\text{cm}^2$  at  $-0.5 \text{ V}$ . For a typical junction, with an area of  $\sim 500 \mu\text{m}^2$ , the tunneling current at  $-0.5 \text{ V}$  would be  $4.2 \times 10^{-13} \text{ A}$ , which is below the detection limit ( $\sim 10^{-12} \text{ A}$ ) of our electrometer. We attempted to measure current densities across SC<sub>19</sub> on different days and using different substrates, but the data were highly inconsistent, and the  $J(V)$  data had a very broad distribution ( $\sigma_{\log} = 0.25-1.12$ ). Attempts to measure the  $J(V)$  characteristics of SC<sub>8</sub> and SC<sub>7</sub> yielded similarly incoherent results. These measurements should not suffer from any limitations imposed by our electrometer; however, SAMs of *n*-alkanethiols shorter than SC<sub>9</sub>, being liquid-like and loosely packed, may suffer from a large density of defects that cause large variations in  $J$ . We are exploring ways to improve and characterize SAMs of these short *n*-alkanethiols.

**Statistically Analyzing Distributions of  $\log(|J|)$ .** Charge transport measurements of *n*-alkanethiols from SC<sub>9</sub> to SC<sub>18</sub> yielded values of  $J$  that were log-normally distributed (Figure 3); that is, the distributions of  $\log(|J|/\text{A}/\text{cm}^2)$  (hereafter written as  $\log(|J|)$  for convenience) approximately fit Gaussian functions, whereas the distributions of  $J$  on a linear scale did not. The shape and width (related to  $\sigma_{\log}$ ) of the distributions does not differ appreciably over the range of applied bias from  $-0.5$  to  $0.5 \text{ V}$  (Figure 4). We describe all further analysis using data for  $V = -0.5 \text{ V}$ , but we are confident that the trends identified in this analysis are valid for other biases in the range measured.

In the Experimental Design section, we make the case for analyzing distributions of  $\log(|J|)$ , as opposed to  $J$ . That section introduces the population mean ( $\mu_{\log}$ ) and standard deviation ( $\sigma_{\log}$ ) of  $\log(|J|)$  and explains how these parameters relate to the distribution of  $J$ . Since knowing the shape of the distributions of  $J$  and  $\log(|J|)$  is vital to performing a correct analysis, we emphasize the importance of collecting enough data to resolve this shape adequately. With the exception of SC<sub>9</sub>, we collected at least 700 data points on at least 21 junctions for every compound (Table 1).

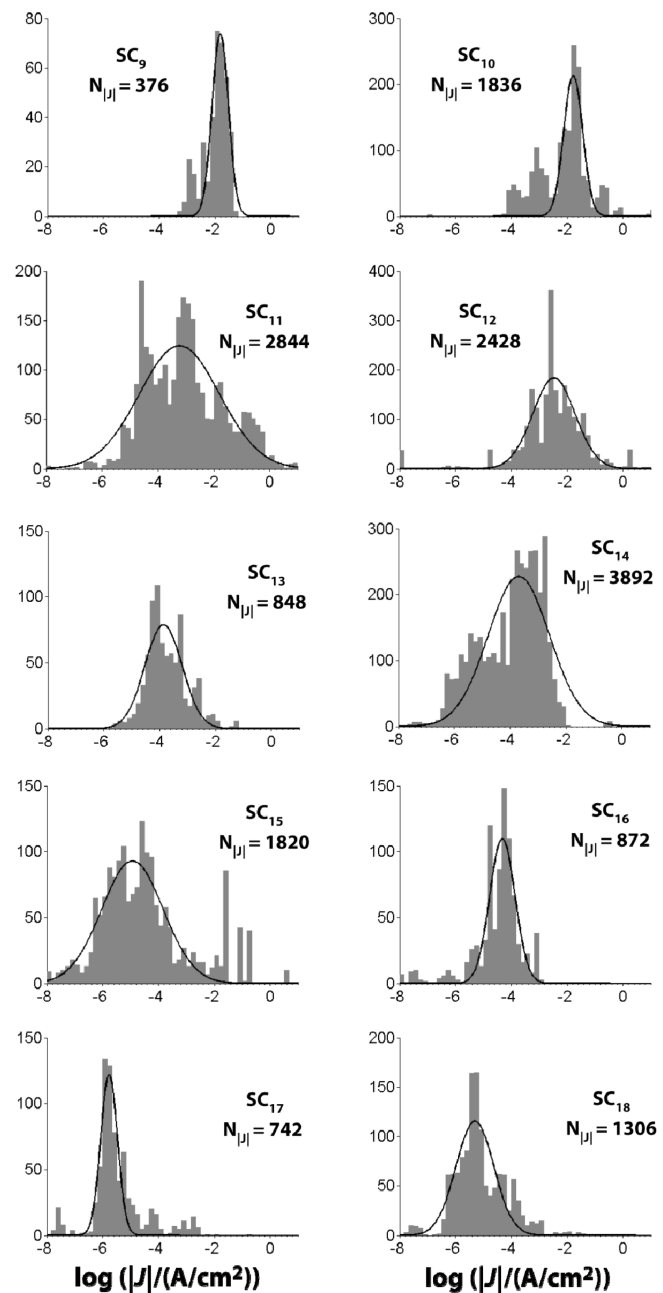


**Figure 3.** Summary of current density,  $J$ , data derived from all *n*-alkanethiols. Histograms of  $\log|J|$  with a Gaussian fit include all the data collected by different users for *n*-alkanethiols (SC<sub>*n*</sub>, where *n* = 9–18);  $N_{|J|}$  is the number of measurements collected for each SAM. A gradual decrease in the current density as chain length increases can be observed from the fitted data. The distributions tend to broaden as the number of data points increases due to slight user-to-user variations.

For an ideal normal distribution of  $\log(|J|)$ ,  $\mu_{\log}$  and  $\sigma_{\log}$  would be trivial to determine; however, our distributions are not ideal and suffer from shorts, outliers, and noise. We define a short as any junction yielding  $\log(|J|) > 2$  (i.e.,  $J > 10^2 \text{ A}/\text{cm}^2$ ; this is approximately 4 orders of magnitude higher than the highest average  $J$  we measured through our most conductive SAM, SC<sub>10</sub>). We do not quantitatively define outliers and noise, but we qualitatively identify the former as values of  $\log(|J|)$  in the histogram that fall well outside of the peak of the Gaussian

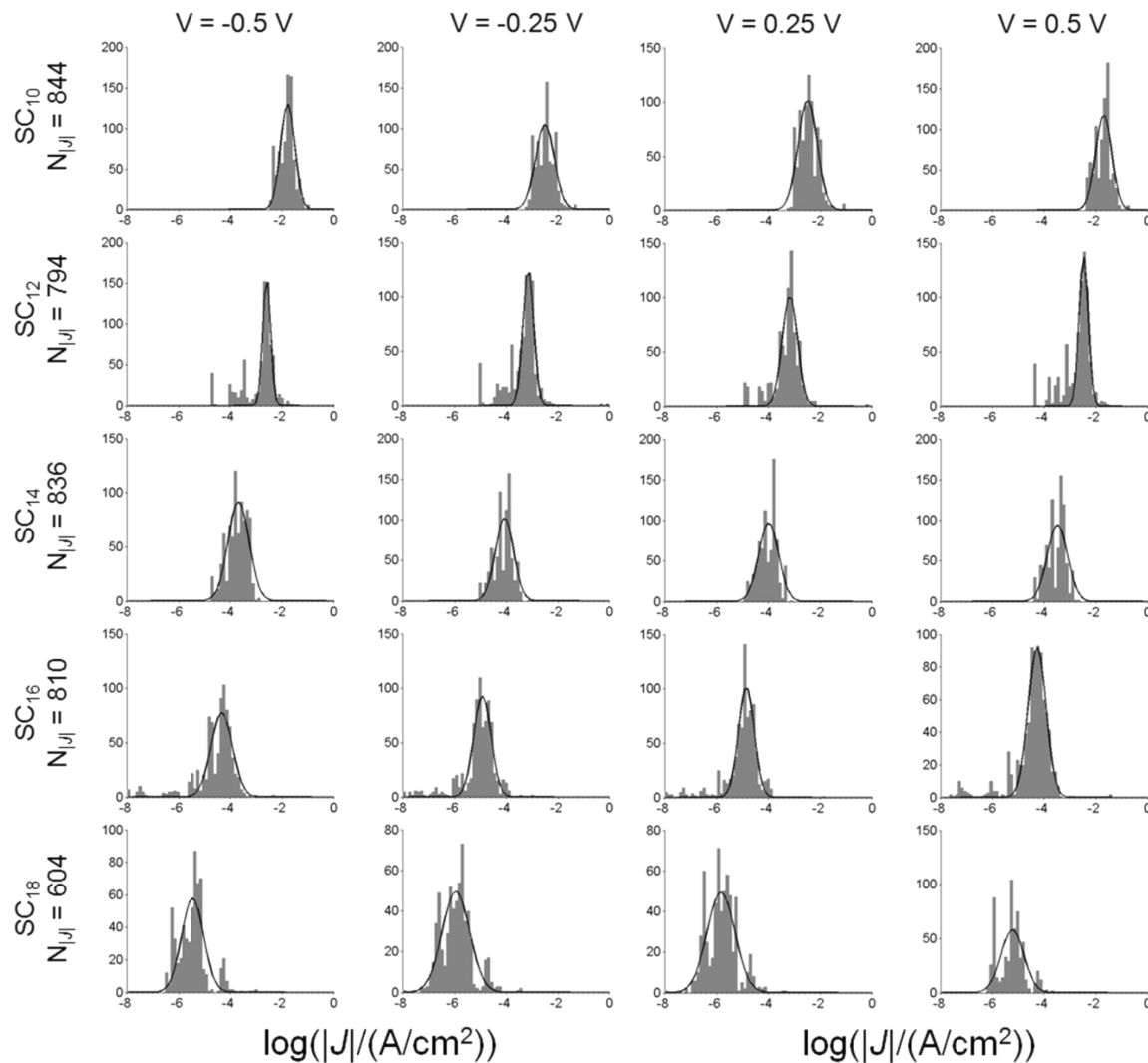


**Figure 4.** Summary of data derived from the even-numbered *n*-alkanethiols at different voltages (from a single user) to illustrate the consistency of the distribution of the data. We show two sets from positive bias and two from negative bias to illustrate that, irrespective of the bias or the voltage ( $|V| = 0.5$  or  $0.25$  V), the histograms look very similar. Similar observations were made with the odd series.

function and the latter as values of  $\log(|J|)$  that cause the shape of the peak to deviate from that of an ideal Gaussian function. For example, we would refer to the counts in the histogram of  $SC_{10}$  (Figure 3) between  $\log(|J|) = -4.5$  and  $-2.5$  as outliers, while we would designate the histogram of  $SC_{14}$  a “noisy” histogram. The distinction between outliers and noise, however, has no bearing on our analysis.

There are two approaches to estimating  $\mu_{\log}$  and  $\sigma_{\log}$  for a nonideal distribution: (i) taking the arithmetic mean and standard deviation of  $\log(|J|)$  and (ii) fitting a Gaussian function to the histogram of  $\log(|J|)$  and extracting the fitting parameters (the mean and standard deviation of the Gaussian). The former approach has the advantage of yielding values of  $\mu_{\log}$  and  $\sigma_{\log}$  that are insensitive to noise, although they are sensitive to shorts and outliers. The latter approach is essentially impervious to shorts and outliers but may be greatly affected by noise. As is evident in Table 2, the estimates of  $\mu_{\log}$  and  $\sigma_{\log}$  obtained using these two approaches can differ by as much as half an order of magnitude. Since the distinction between noise and outliers hinges on the parameters of the Gaussian fit, evaluating which approach to use

can be difficult. Because of the dramatic influence of shorts on the arithmetic mean and standard deviation of  $\log(|J|)$ , however, we elected to work with values of  $\mu_{\log}$  and  $\sigma_{\log}$  determined using the Gaussian fit. Figure 3 shows Gaussian fits to the histograms of  $\log(|J|)$ . Table 2 reports the values of  $\mu_{\log}$  and  $\sigma_{\log}$  determined both ways and shows that, for all SAMs except  $SC_{10}$  and  $SC_{17}$ , more than 80% of the values of  $\log(|J|)$  fall within the interval of  $\mu_{\log} \pm 3 \sigma_{\log}$  determined by the Gaussian fit. We will discuss the rationale and implications of the choice to fit Gaussians, rather than to calculate the arithmetic mean and standard deviation, in detail in a separate paper.<sup>143</sup>

As noted above, we attribute the log-normal distribution of  $J$  to a normal distribution of the distance between the top and bottom electrodes. According to the simplified Simmons relation (eq 1),  $J$  is exponentially dependent on  $d$ . We hypothesize that the nature of defects on the SAM — a number of different types of defects, randomly distributed — leads to a normal distribution of  $d$ , which, in turn, implies a normal distribution of  $\log(|J|)$ .

**The SAM Is at Least Partially Responsible for the Random Error in  $J$ .** It is instructive to note the differences in  $\sigma_{\log}$  across

**Table 2.** Comparison of Methods for Determining the Population Mean of  $\log(|J|)$ 

$n$	$\mu_{\log} \pm \sigma_{\log}$	Gaussian fit <sup>b</sup>	data within Gaussian (%) <sup>c</sup>
9	$-1.99 \pm 0.45$	$-1.78 \pm 0.29$	87
10	$-2.12 \pm 1.0$	$-1.77 \pm 0.32$	60
11	$-3.04 \pm 1.4$	$-3.23 \pm 1.44$	94
12	$-2.54 \pm 1.3$	$-2.47 \pm 0.77$	89
13	$-3.73 \pm 0.74$	$-3.86 \pm 0.66$	95
14	$-4.01 \pm 1.1$	$-3.70 \pm 1.1$	99
15	$-4.45 \pm 1.6$	$-4.93 \pm 1.1$	88
16	$-4.51 \pm 0.90$	$-4.32 \pm 0.45$	92
17	$-5.46 \pm 0.98$	$-5.81 \pm 0.23$	73
18	$-5.08 \pm 0.93$	$-5.31 \pm 0.66$	93

<sup>a</sup> Calculated by taking the arithmetic average and standard deviation of  $\log(|J|)$  after excluding shorts. <sup>b</sup> The parameters of the Gaussian function that was the least-squares fit to the histogram of  $\log(|J|)$ . No data were excluded. <sup>c</sup> Defined as the percentage of values of  $\log(|J|)$  that lie within 3 standard deviations above and below the mean (mean and standard deviation determined from the Gaussian fit).

the series of  $n$ -alkanethiols. According to Table 2, this parameter, in log units, ranges from 0.45 to 1.6 when calculated as the arithmetic standard deviation of  $\log(|J|)$  and from 0.29 to 1.1 when determined by fitting a Gaussian. No unambiguous trend in  $\sigma_{\log}$  vs  $d$  emerges from the data, but  $\sigma_{\log}$  does appear to be smaller at the extremes of the series and larger in the middle (especially SC<sub>14</sub> and SC<sub>15</sub>). Since the substrate and top electrode remain invariant across the series of  $n$ -alkanethiols, the large range in  $\sigma_{\log}$  is due to the SAM and not the roughness of the Ag<sup>Ts</sup> electrode or variations in the morphology, composition, or electrical properties of the Ga<sub>2</sub>O<sub>3</sub>/EGaIn electrode. We therefore believe that, despite the presence of incompletely defined components in our system, our measurements are sensitive to the properties of the SAM and useful for studying charge transport in organic matter.

**Demonstrating the Odd–Even Effect.** Figure 5 summarizes the results of fitting all the distributions of  $\log(|J|)$  for  $n$ -alkanethiols. In the right column of Figure 5, we show the population mean of  $J, \mu_J$  (with error bars defined by  $\sigma_J$ ) vs chain length at  $V = -0.5$  V for odd-numbered, even-numbered, and all alkanethiols, respectively. Similarly, in the left column of Figure 5, we show  $\mu_J$  vs applied bias (constituting an average  $J(V)$  trace) for the same groupings of alkanethiols. For the odd- and even-numbered alkanethiols plotted separately,  $\mu_J$  decreases exponentially with increasing chain length. However, in the combined data set, the visible oscillation between increasing and decreasing  $\mu_J$  suggests a measurable difference in charge transport between odd- and even-numbered  $n$ -alkanethiols.

The issue of whether there is such an “odd–even effect”, or just noise in a simple progression of  $J$  with chain length, revolves around the question of whether the odd- and even-numbered alkanethiols are best regarded as two separate data sets requiring distinct analyses or as one coherent data set adequately described by parameters in common. Here, we give two simple, statistical justifications for regarding the odd- and even-numbered alkanethiols as two separate data sets (we will discuss other, more complex reasons and statistical data in a separate paper).<sup>39,53,132,134</sup>

(i) When considered as separate data sets, both the odd- and even-numbered alkanethiols exhibit an uninterrupted decrease in

$\log(|J|)$  with increasing chain length, but when they are collected in a single data set, this trend breaks down. Using a two-sample *t* test, it is possible to compare two normally distributed samples to determine whether the samples come from populations with significantly different means and to evaluate which of the means is greater. For example, comparing  $\log(|J|(-0.5\text{ V}))$  between SC<sub>10</sub> and SC<sub>12</sub> using a *t* test leads to the conclusion, at the 99% confidence level, that  $\mu_{\log, \text{SC}_{10}} > \mu_{\log, \text{SC}_{12}}$ . It is important to note that the *t* test assumes that the data being analyzed are normally distributed; thus, it is important to work with distributions of  $\log(|J|)$ , and not  $J$ , for this analysis. Applying the *t* test separately to the two series of odd- and even-numbered alkanethiols yields the following two sets of inequalities, valid at the 99% confidence level:

$$\mu_{\log, \text{SC}_9} > \mu_{\log, \text{SC}_{11}} > \mu_{\log, \text{SC}_{13}} > \mu_{\log, \text{SC}_{15}} > \mu_{\log, \text{SC}_{17}} \quad (2)$$

$$\mu_{\log, \text{SC}_{10}} > \mu_{\log, \text{SC}_{12}} > \mu_{\log, \text{SC}_{14}} > \mu_{\log, \text{SC}_{16}} > \mu_{\log, \text{SC}_{18}} \quad (3)$$

For both data sets, the trend of decreasing  $\mu_{\log}$  with increasing chain length is statistically significant and unbroken. Applying the *t* test to the combined data set of odd- and even-numbered alkanethiols, however, yields a different set of inequalities (see Table 2):

$$\begin{aligned} \mu_{\log, \text{SC}_9} &\approx \mu_{\log, \text{SC}_{10}} > \mu_{\log, \text{SC}_{11}} < \mu_{\log, \text{SC}_{12}} > \mu_{\log, \text{SC}_{13}} < \mu_{\log, \text{SC}_{14}} \\ &> \mu_{\log, \text{SC}_{15}} < \mu_{\log, \text{SC}_{16}} > \mu_{\log, \text{SC}_{17}} < \mu_{\log, \text{SC}_{18}} \end{aligned} \quad (4)$$

The symbol “≈” indicates that the *t* test could not distinguish between the population means of  $\log(|J|(-0.5\text{ V}))$  for SC<sub>9</sub> and SC<sub>10</sub> at the 99% confidence level. While the values of  $\mu_{\log}$  generally decrease with increasing chain length, the  $\mu_{\log}$  of every odd alkanethiol is less than the  $\mu_{\log}$  of the even alkanethiol with one more methylene (even though the former is shorter than the latter). The alternating direction of the inequalities is a clear deviation from the trend observed in the separate odd and even data sets and, thus, constitutes one piece of evidence for an odd–even effect.

(ii) Linear regression of  $\log(|J|)$  vs chain length indicates that the odd- and even-numbered alkanethiols belong to two separate data sets. As noted above, the rate of charge transport through SAMs of alkanethiols decays exponentially with increasing chain length, such that the relationship between  $\log(|J|)$  and  $d$  is linear ( $\log(|J|) = \log(J_0) - \log(e)\beta d$ ). Linear least-squares fitting of  $\log(|J|)$  vs  $d$  gives estimates for the parameters  $J_0$  and  $\beta$  (discussed below) and determines the region that is 95% likely to contain the true fit (this region is bounded by so-called 95% confidence bands).<sup>144</sup> We performed two separate linear fits of  $\mu_{\log}$  vs  $d$  for odd- and even-numbered alkanethiols using the estimates of  $\mu_{\log}$  at  $V = -0.5$  V determined by fitting Gaussian functions to the histograms of  $\log(|J|(-0.5\text{ V}))$ , as described above.<sup>145</sup> Figure 6 shows these fits, along with their 95% confidence bands. A key feature of this plot is that the 95% confidence bands for the two fits do not overlap in the region between SC<sub>11</sub> and SC<sub>18</sub> (though they do overlap outside this region, see below). While we cannot claim, with statistical confidence, any difference in  $J_0$  or  $\beta$  (see below) between the odd- and even-numbered alkanethiols, we can state, with 95% confidence, that two separate lines fit the combined data set of odd- and even-numbered alkanethiols better than any single line. In other words, the odd- and even-numbered alkanethiols are best regarded as distinct data sets, due to the presence of an odd–even effect resulting from an as-yet unidentified cause.

**Explaining the Odd–Even Effect.** Given an odd-numbered alkanethiol and the corresponding even-numbered alkanethiol

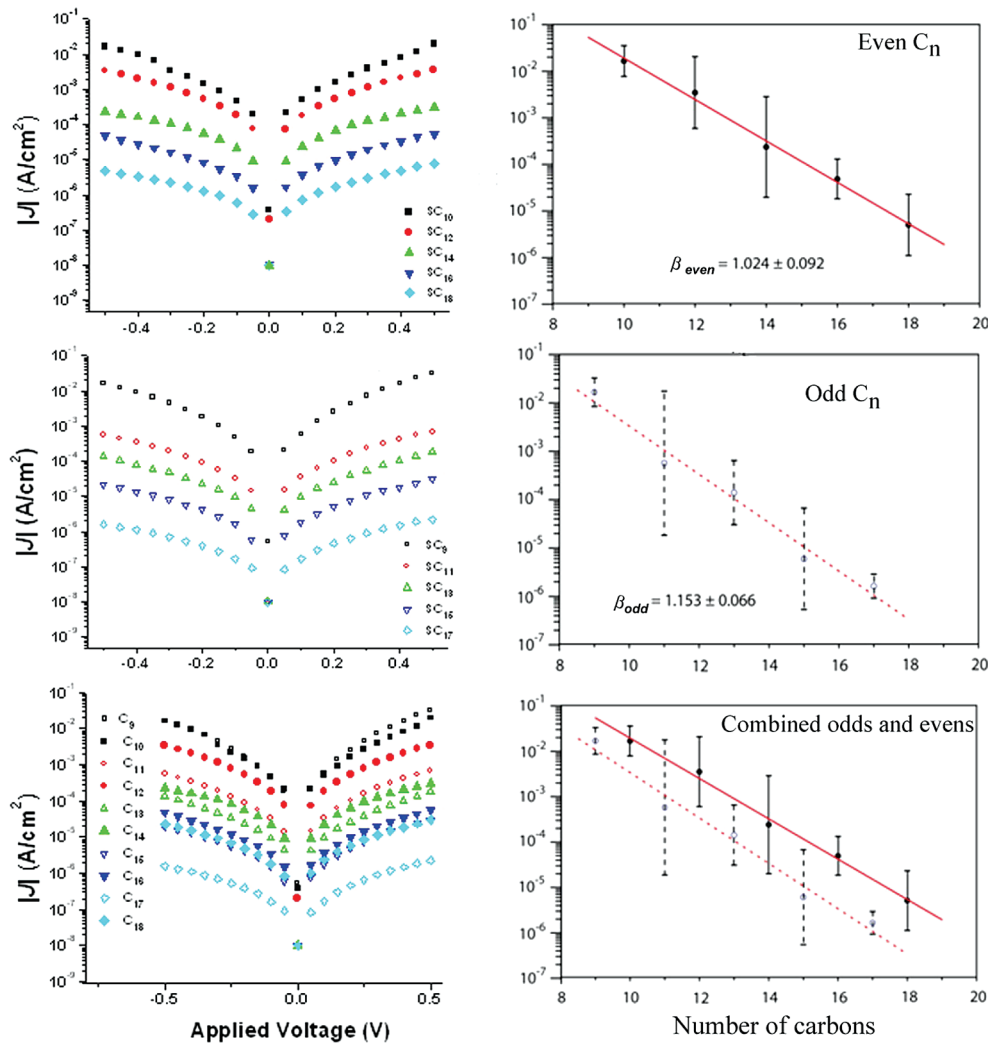


**Figure 5.** Plot of  $\ln|J|$  (V) at  $-0.5$  V against the chain length of the  $n$ -alkanethiols, given in number of carbons, for all SAMs studied. Each point corresponds to the mean of the Gaussian fit to the histograms above (Figures 3), and the error bars represent the log-standard deviation. SAMs derived from even  $n$ -alkanethiols gave higher current densities than the analogous odd series. For each series of  $n$ -alkanethiols—odd or even—the corresponding average  $J(V)$  curves are given next to the plot of current densities at  $-0.5$  V.

with one more methylene, it is surprising that the current density through the shorter (odd) alkanethiol is always less than the current density through the longer (even) alkanethiol (e.g.,  $\mu_{\log C_{11}} < \mu_{\log C_{12}}$ ). This (statistically verified) observation contradicts the prediction of the Simmons model (eq 1) under the assumptions that  $\beta$  and  $J_0$  are the same for odd- and even-numbered alkanethiols. Clearly, either one or both of the assumptions are wrong, or the Simmons model lacks the power to account for the odd–even effect.

In order to decide this question, we attempted to determine  $\beta$  and  $J_0$  for the odd- and even-numbered alkanethiols separately. Fitting each of these two data sets (data taken by several experimentalists, Figure 5a,b) to eq 1 gives two values for the tunneling decay constant:  $\beta_{\text{odd}} = 1.15 \pm 0.07 n_C^{-1}$  and  $\beta_{\text{even}} = 1.02 \pm 0.09 n_C^{-1}$  at  $-0.5$  V. Considering the error in these estimates, we stress that the difference in these two values is not statistically significant, so we can neither conclude that they are the same nor that they are different. Comparing these data with data taken by a single user (Figure 7), we observe  $\beta_{\text{odd}} = 1.19 \pm 0.08 n_C^{-1}$  and  $\beta_{\text{even}} = 1.05 \pm 0.06 n_C^{-1}$  at  $-0.5$  V. These

values are also indistinguishable due to error. Our value of  $\beta$  for the even-numbered  $n$ -alkanethiols occupies the high end of the range of values reported for systems using Hg-SAM electrodes and spin-cast polymer electrodes ( $\beta_{\text{even}} = 0.71$ – $1.1 n_C^{-1}$ ).<sup>62,66,77,146</sup>–<sup>149</sup>

Likewise, the separate fits to eq 1 of data from odd- and even-numbered alkanethiols give two log-normally distributed estimates for the pre-exponential factor:  $\log(|J_{0,\text{odd}}|) = 2.42 \pm 0.68$  (i.e.,  $|J_{0,\text{odd}}| = 2.6 \times 10^2 \text{ A/cm}^2$  with a 95% confidence interval of  $1.1 \times 10$ – $6.0 \times 10^3 \text{ A/cm}^2$ ) and  $\log(|J_{0,\text{even}}|) = 2.73 \pm 0.54$  (i.e.,  $|J_{0,\text{even}}| = 5.4 \times 10^2 \text{ A/cm}^2$  with a 95% confidence interval of  $4.5 \times 10$ – $6.5 \times 10^3 \text{ A/cm}^2$ ). Note that, in Figure 6, the 95% confidence bands for the two linear fits do not overlap in the region containing the bulk of the data but do substantially overlap when the fits are extrapolated to  $n_C = 0$  in order to determine  $J_0$ . Again, we emphasize that the magnitude of the error in these estimates makes it impossible to say, with statistical confidence, whether  $J_{0,\text{odd}}$  and  $J_{0,\text{even}}$  are the same or different. The lack of reported values of  $J_0$  in the literature makes direct comparisons of this value across experimental platforms difficult.

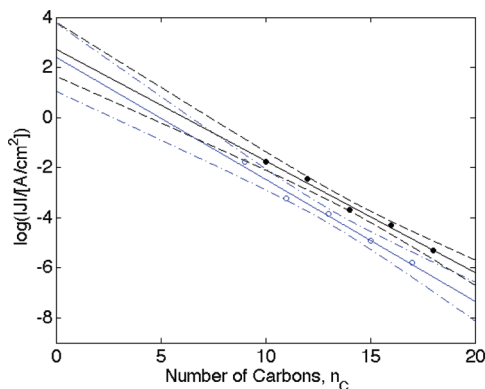


**Figure 6.** Plot of  $\mu_{\log}$  vs chain length for odd (open blue circles) and even (solid black circles) alkanethiols. The solid lines are the best linear, least-squares fits to the odd (blue) and even (black) data. Dot-dashed blue lines represent the 95% confidence bands for the fit to the odd-numbered alkanethiols, and dashed black lines show the 95% confidence bands for the fit to the even-numbered alkanethiols. Error bars have been omitted for clarity. The two 95% confidence bands do not overlap in the region of SC<sub>11</sub> through SC<sub>18</sub>, indicating that two different fits are warranted. The confidence bands do, however, overlap outside of this region, especially as the extrapolated fit approaches  $n_C = 0$ . Distinguishing between the slopes (related to  $\beta$ ) and intercepts (related to  $J_0$ ) of the two fits is, thus, difficult.

The noise in our data, and the limited power of our statistical analysis, cannot distinguish between the values of  $\beta_{\text{odd}}$  and  $\beta_{\text{even}}$ , nor between  $J_{0,\text{odd}}$  and  $J_{0,\text{even}}$ . The fact that we cannot prove that these values are different, however, does not imply that they are the same. Indeed, as techniques improve and measurements become more precise, a statistically significant difference in  $\beta$  or  $J_0$  may still emerge. Since  $\beta$  is related to the shape and height of the tunneling barrier, statistically proving that  $\beta_{\text{odd}} > \beta_{\text{even}}$  would imply that odd-numbered alkanethiols present a tunneling barrier with a significantly different shape and/or height than do even-numbered alkanethiols. Meanwhile,  $J_0$  captures the effect of all interfaces (the covalent Ag–S interface and the noncovalent SAM//Ga<sub>2</sub>O<sub>3</sub> interface) and components (EGaIn, Ga<sub>2</sub>O<sub>3</sub>, and Ag) aside from the SAM itself. The only item in this list that varies between odd- and even-numbered alkanethiols is the SAM//Ga<sub>2</sub>O<sub>3</sub> interface: in a *trans*-extended odd-numbered alkanethiol, the terminal C–C bond is roughly vertical and the terminal methyl group is the only group in contact with Ga<sub>2</sub>O<sub>3</sub>, while in a *trans*-extended even-numbered alkanethiol, the terminal C–C bond is more horizontal and the terminal ethyl group is in contact with the Ga<sub>2</sub>O<sub>3</sub> layer. Statistical confirmation that  $J_{0,\text{odd}} < J_{0,\text{even}}$  would imply that charge injection is more favorable at the ethyl//Ga<sub>2</sub>O<sub>3</sub> interface than at the methyl//Ga<sub>2</sub>O<sub>3</sub> interface.

However, since we cannot statistically confirm any differences between  $\beta$  and  $J_0$  for odd- and even-numbered alkanethiols, there is also the possibility that the Simmons model lacks the power to explain the odd–even effect. It is possible that a model with a different functional form than eq 1, or with additional parameters, would better describe tunneling through SAMs than the Simmons model. Since Simmons originally developed the model to describe tunneling through solid-state, inorganic films, this possibility is not out of the question.

**Reproducibility.** There are two axes along which to assess the reproducibility of measurements using Ag<sup>TS</sup>-SC<sub>n</sub>//Ga<sub>2</sub>O<sub>3</sub>/EGaIn junctions: dependence on the technique of the operator and dependence on the ambient conditions of measurement.

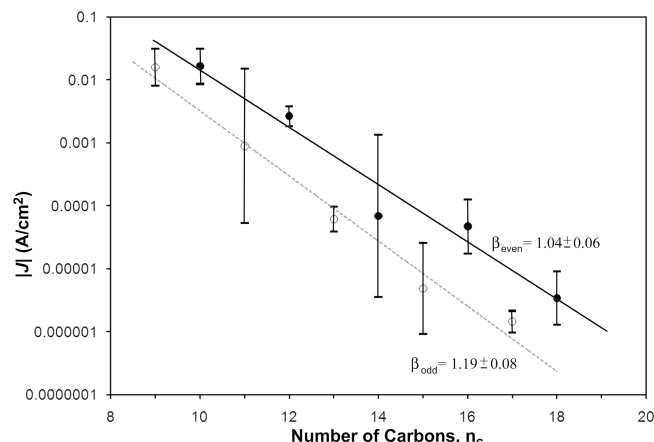


**Figure 7.** Plot of  $\ln|J|$  (V) at  $-0.5$  V against the chain length of the alkanethiols, given in number of carbons, for all SAMs as measured by a single user across either the odd- or even-numbered *n*-alkanethiols. The observed values of  $\beta$  from single users are not significantly different from those obtained from measurements of a group of five users.

Like any manual technique, the formation of conical tips of Ga<sub>2</sub>O<sub>3</sub>/EGaIn, and the formation of tunneling junctions using these tips, is an operator-dependent process.

Some parameters — notably, the speed with which an operator retracts the syringe to form the tip, the tolerance of the operator for deviations of the shape of the tip from the “ideal”, and the force with which an operator applies the tip to the SAM — are difficult to quantify and even more difficult to standardize across operators. Further, as we have noted above, the surface of the Ga<sub>2</sub>O<sub>3</sub> is likely contaminated with a thin film of adsorbed organic material, and it is likely that the composition and thickness of this film depend on the local environment at the time of measurement.

While we are currently pursuing strategies to minimize operator dependence (through standardized formation of electrodes) and environmental dependence (by isolating the measurement stage in a chamber with a controlled atmosphere), the measurements described here are sufficiently reproducible to lend confidence to our conclusions.

We point to two pieces of evidence to demonstrate the reproducibility of our results: the similarity of distributions of  $\log(|J|)$  collected by multiple users for individual compounds and the similarity of values of  $\beta$  calculated by a single user vs multiple users.

Figure 8 shows the contributions of three different operators to the data set of  $\log(|J|)$  for SC<sub>18</sub> at  $V = -0.5$  V (though it is typical of all compounds and all values of applied bias). These operators collected their data on different days under different ambient conditions. The histograms from individual users (color) are normal distributions of  $\log(|J|)$  that collectively sum to the normal distribution of all values of  $\log(|J|)$  (gray). The distribution from user 1 has  $\mu_{\log} = -4.65 \pm 0.61$ , that from user 2 has  $\mu_{\log} = -5.44 \pm 0.41$ , and that from user 3 has  $\mu_{\log} = -5.24 \pm 0.97$ , as determined from fitting Gaussian functions to the histograms (see Table S2 in the Supporting Information). While the means of these distributions are not identical, the error bars on these means do overlap substantially. Two-sample *t* tests confirm that there is no statistically significant difference between the distributions from users 1 and 2 ( $p = 0.16$ ) and from users 1 and 3 ( $p = 0.16$ ). Interestingly, the test did find a statistically

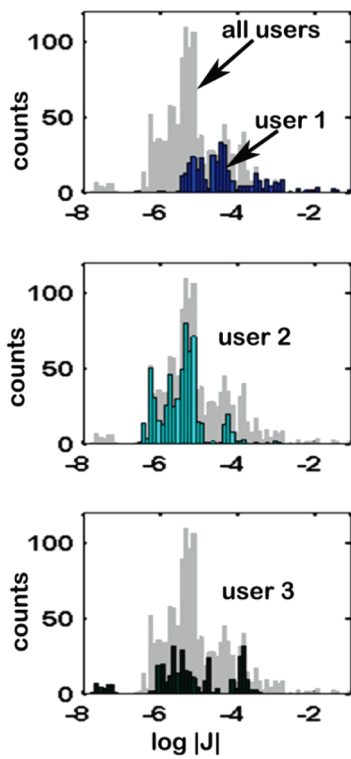


**Figure 8.** Histograms of data collected for the octadecanethiol SAM from three different users. Data from a single analyst are shown with the pooled data from all users in the background (gray). These figures are representative of all compounds in both series (odd and even).

significant difference between users 2 and 3 ( $p \ll 0.01$ ), but this may be due to the cluster of outliers, near  $\log(|J|) = -4.0$ , in the distribution of user 3. In any case, the variations between operators serve to broaden the overall distribution of  $\log(|J|)$  for each compound but do not preclude statistical comparisons across different compounds, as demonstrated above.

It is instructive to compare entire data sets, and not just single compounds, collected by a single user within a short time frame (<1 week) and by multiple users over a long time frame (>1 month). Figure 5 shows data for  $\text{SC}_9$  through  $\text{SC}_{18}$  collected by a total of six users, along with values for  $\beta_{\text{even}}$  and  $\beta_{\text{odd}}$ . By contrast, Figure 6 shows data for odd-numbered alkanethiols, collected by a single user, and for even-numbered alkanethiols, collected by a different individual (independently, both data sets derive from a single user). The error bars are generally smaller for the single-user data sets than for the data sets collected by multiple users; as noted above, however, the values of  $\beta$  determined for corresponding data sets are indistinguishable. Despite the evident challenges to reproducible formation of  $\text{Ga}_2\text{O}_3/\text{EGaIn}$  tips and measurement of tunneling junctions, therefore, we conclude that the reproducibility of these measurements is sufficient to draw conclusions with confidence from trends in the data.

## CONCLUSIONS

Measurements using  $\text{Ag}^{\text{TS}}\text{-}\text{SC}_n//\text{Ga}_2\text{O}_3/\text{EGaIn}$  junctions demonstrated a difference in rates of charge transport through SAMs with odd- and even-numbered *n*-alkanethiols. The sensitivity of this technique to the subtle differences in the structure of the SAM and its interface with the  $\text{Ga}_2\text{O}_3$  layer arises from at least

four factors: (i) the use of ultraflat metal surfaces ( $\text{Ag}^{\text{TS}}$ ) to fabricate the SAMs, (ii) the careful purification of the *n*-alkanethiols used to form SAMs, (iii) the presence, on the  $\text{Ga}_2\text{O}_3/\text{EGaIn}$  top electrode, of a thin (~2 nm) layer of oxide that protected the junction from artifacts and shorts while not interfering with charge transport, and (iv) the application of statistical analysis to a large number of measurements.

Though the  $\text{Ga}_2\text{O}_3/\text{EGaIn}$  electrode has both advantages and disadvantages, it is demonstrably useful for physical–organic studies of charge transport.  $\text{Ag}^{\text{TS}}\text{-SAM}/\text{Ga}_2\text{O}_3/\text{EGaIn}$  junctions exhibit high yield (>80%) and, thus, allow for the collection of large amounts of data within a short time. These junctions do not require a cleanroom, an ultrahigh vacuum, toxic substances such as Hg, a solvent bath, or a second SAM. They do, however, require a skilled user and attention to detail in order to yield meaningful results, primarily (we believe) because the formation of conical tips of  $\text{Ga}_2\text{O}_3/\text{EGaIn}$  is a user-dependent process. We are working on determining and eliminating the elements of our procedure that contribute to this user dependence and thus standardizing the procedure.

The least well-defined component of this system is the thin (~2 nm) layer of  $\text{Ga}_2\text{O}_3$  on the surface of the electrode, along with any organic material adsorbed on its surface. On one hand, this film of  $\text{Ga}_2\text{O}_3$ , like protective layers in other techniques, helps to prevent the formation of metal filaments, and so we believe that this layer is necessary to achieve high yields of working junctions. On the other hand, the morphology and electrical properties of the layer of  $\text{Ga}_2\text{O}_3$  are not completely defined and are possibly sensitive to how the electrode is formed. On the basis of the observation that the width of the distribution of  $J$  varies across the series of SAMs investigated, we conclude that the SAM contributes at least as significantly to the random error in our measurements as the layer of  $\text{Ga}_2\text{O}_3$ .

While odd–even effects have been reported in studies of the properties of *n*-alkanethiols, the observation of an odd–even effect in the context of charge transport is important for two reasons: (i) it demonstrates that the  $\text{Ag}^{\text{TS}}\text{-}\text{SC}_n//\text{Ga}_2\text{O}_3/\text{EGaIn}$  junction measures properties of SAMs (as opposed to artifacts of the electrodes), and (ii) it provides a test for theoretical descriptions of charge transport through SAMs.

While we were able to identify an odd–even effect with respect to  $J$ , the random error in our measurements was too large to reveal whether there was a statistically significant difference in the tunneling decay constant,  $\beta$ , or the pre-exponential factor,  $J_0$ , between odd- and even-numbered alkanethiols. We stress that we cannot pinpoint the origin of the odd–even effect. We can, however, identify some possibilities. (i) Further experiments may distinguish between  $\beta_{\text{odd}}$  and  $\beta_{\text{even}}$  and imply that a significant difference in the electronic structure of odd- and even-numbered alkanethiols exists and affects the shape and/or height of the tunneling barrier posed by the SAM. (ii) Alternatively, further experiments may locate the origin of the odd–even effect in  $J_0$ , implying that methyl- and ethyl-terminated surfaces lead to significantly different interfaces, with respect to charge transport. (iii) Finally, the odd–even effect may point to a deficiency in the Simmons model as a description of charge transport through SAMs. Due to the current limitations of our experimental methods and statistical analysis, we decline to speculate on which of these possibilities is most likely, in order to avoid biasing further investigations in the field.

The measured values of the tunneling decay constant — $\beta_{\text{odd}} = 1.15 \pm 0.07 \text{ } n_{\text{C}}^{-1}$  for even-numbered alkanethiols and  $\beta_{\text{even}} = 1.02 \pm 0.09 \text{ } n_{\text{C}}^{-1}$  for odd-numbered alkanethiols — both lie

within, but at the high end of, the range of values reported in the literature ( $0.75\text{--}1.1 n_{\text{C}}^{-1}$ ). Again, we stress that the difference between the *measured* values of  $\beta_{\text{even}}$  and  $\beta_{\text{odd}}$  is not statistically significant.

## ■ ASSOCIATED CONTENT

**S Supporting Information.** Experimental details, Tables S1 and S2, and NMR spectra. This material is available free of charge via the Internet at <http://pubs.acs.org>.

## ■ AUTHOR INFORMATION

### Corresponding Author

gwhitesides@gmwgroup.harvard.edu

## ■ ACKNOWLEDGMENT

This work was funded by NSF grant (grant CHE-05180055) to G.M.W. M.M. and J.B. were supported by a Mary-Fieser postdoctoral fellowship and the NanoScience and Engineering Centre (NSEC) at Harvard University. The Netherlands Organization for Scientific Research (NWO) is kindly acknowledged for the Rubicon grant to C.A.N. Singapore National Research Foundation is kindly acknowledged for funding (NRF Award No. NRF-RF2010-03) to C.A.N.

## ■ REFERENCES

- (1) Reus, W. F.; Nijhuis, C. A.; Barber, J. R.; Mwangi, M. T.; Cademartiri, L.; Kim, C.; York, R. L.; Liu, X.; Whitesides, G. M. *Harvard University*, 2010, unpublished.
- (2) Tao, F.; Bernasek, S. L. *Chem. Rev.* **2007**, *107*, 1408.
- (3) Love, J. C.; Estroff, L. A.; Kriebel, J. K.; Nuzzo, R. G.; Whitesides, G. M. *Chem. Rev.* **2005**, *105*, 1103.
- (4) Nishi, N.; Hobara, D.; Yamamoto, M.; Kakiuchi, T. *J. Chem. Phys.* **2003**, *118*, 1904.
- (5) Bai, B.; Wang, H.; Xin, H.; Long, B.; Li, M. *Liq. Cryst.* **2007**, *34*, 659.
- (6) Blumstein, A.; Blumstein, R. B. *Recent Adv. Liq. Cryst. Polym., [Proc. Eur. Sci. Found. Polym. Workshop Liq. Cryst. Polym. Syst., 6th]* **1985**, 129.
- (7) Blumstein, A.; Thomas, O. *Macromolecules* **1982**, *15*, 1264.
- (8) Cacelli, I.; De Gaetani, L.; Prampolini, G.; Tani, A. *Mol. Cryst. Liq. Cryst.* **2007**, *465*, 175.
- (9) Capar, M. I.; Cebe, E. *Phys. Rev. E: Stat., Nonlinear, Soft Matter Phys.* **2006**, *73*, 061711/1.
- (10) Capar, M. I.; Cebe, E. *J. Comput. Chem.* **2007**, *28*, 2140.
- (11) Centore, R. *Liq. Cryst.* **2009**, *36*, 239.
- (12) Chang, H.-S.; Wu, T.-Y.; Chen, Y. *J. Appl. Polym. Sci.* **2002**, *83*, 1536.
- (13) Cheng, S. Z. D.; Li, C. Y.; Jin, S.; Weng, X.; Zhang, D.; Bal, F.; Zhang, J. Z.; Harris, F. W.; Chien, L.-C.; Lotz, B. *PMSE Prepr.* **2003**, *89*, 88.
- (14) Dunn, C. J.; Le Masurier, P. J.; Luckhurst, G. R. *Phys. Chem. Chem. Phys.* **1999**, *1*, 3757.
- (15) Haegele, C.; Wuckert, E.; Laschat, S.; Giesselmann, F. *ChemPhysChem* **2009**, *10*, 1291.
- (16) Henderson, P. A.; Cook, A. G.; Imrie, C. T. *Liq. Cryst.* **2004**, *31*, 1427.
- (17) Henderson, P. A.; Inkster, R. T.; Seddon, J. M.; Imrie, C. T. *J. Mater. Chem.* **2001**, *11*, 2722.
- (18) Itahara, T.; Tamura, H. *Mol. Cryst. Liq. Cryst.* **2007**, *474*, 17.
- (19) Johannsmann, D.; Zhou, H.; Sonderkaer, P.; Wierenga, H.; Myrvold, B. O.; Shen, Y. R. *Phys. Rev. E: Stat. Phys., Plasmas, Fluids, Relat. Interdiscip. Top.* **1993**, *48*, 1889.
- (20) Kobayashi, K.; Yoshizawa, A. *Liq. Cryst.* **2007**, *34*, 1455.
- (21) Kundu, B.; Pal, S. K.; Kumar, S.; Pratibha, R.; Madhusudana, N. V. *Europhys. Lett.* **2009**, *85*, 36002/1.
- (22) Marcelis, A. T. M.; Koudijs, A.; Sudhoelter, E. J. R. *Thin Solid Films* **1996**, *284*–*285*, 308.
- (23) Noack, F. *Mol. Cryst. Liq. Cryst.* **1984**, *113*, 247.
- (24) Ojha, D. P.; Kumar, D.; Pisipati, V. G. K. M. *Cryst. Res. Technol.* **2002**, *37*, 881.
- (25) Ojha, D. P.; Kumar, D.; Pisipati, V. G. K. M. *Z. Naturforsch., A: Phys. Sci.* **2002**, *57*, 189.
- (26) Parri, O.; Coates, D.; Greenfield, S.; Goulding, M.; Verrall, M. *Mol. Cryst. Liq. Cryst. Sci. Technol., Sect. A* **1999**, *332*, 2783.
- (27) Roviello, A.; Sirigu, A. *Makromol. Chem.* **1982**, *183*, 895.
- (28) Stals, P. J. M.; Smulders, M. M. J.; Martin-Rapun, R.; Palmans, A. R. A.; Meijer, E. W. *Chem.—Eur. J.* **2009**, *15*, 2071.
- (29) Umadevi, S.; Jakli, A.; Sadashiva, B. K. *Soft Matter* **2006**, *2*, 875.
- (30) Umamaheswari, U.; Ajeetha, N.; Srinivas, G.; Ojha, D. P. *Bull. Pure Appl. Sci., Sect. D* **2008**, *27D*, 55.
- (31) Yamaguchi, A.; Watanabe, M.; Yoshizawa, A. *Liq. Cryst.* **2007**, *34*, 633.
- (32) Yoshizawa, A.; Chiba, S.; Ogasawara, F. *Liq. Cryst.* **2007**, *34*, 373.
- (33) Yung, K. L.; He, L.; Xu, Y.; Shen, Y. W. *J. Chem. Phys.* **2005**, *123*, 246101/1.
- (34) Azzam, W.; Cyganik, P.; Witte, G.; Buck, M.; Woell, C. *Langmuir* **2003**, *19*, 8262.
- (35) Kato, H. S.; Noh, J.; Hara, M.; Kawai, M. *J. Phys. Chem. B* **2002**, *106*, 9655.
- (36) Kobayashi, T.; Seki, T. *Langmuir* **2003**, *19*, 9297.
- (37) Shaporenko, A.; Brunnbauer, M.; Terfort, A.; Johansson, L. S. O.; Grunze, M.; Zharnikov, M. *Langmuir* **2005**, *21*, 4370.
- (38) Wintgens, D.; Yablon, D. G.; Flynn, G. W. *J. Phys. Chem. B* **2003**, *107*, 173.
- (39) Stolar, P.; Kshirsagar, R.; Massi, M.; Annibale, P.; Albonetti, C.; de Leeuw, D. M.; Biscarini, F. *J. Am. Chem. Soc.* **2007**, *129*, 6477.
- (40) Auer, F.; Nelles, G.; Sellergren, B. *Chem.—Eur. J.* **2004**, *10*, 3232.
- (41) Heimel, G.; Romaner, L.; Bredas, J.-L.; Zojer, E. *Langmuir* **2008**, *24*, 474.
- (42) Kikkawa, Y.; Koyama, E.; Tsuzuki, S.; Fujiwara, K.; Miyake, K.; Tokuhisa, H.; Kaneko, M. *Chem. Commun.* **2007**, 1343.
- (43) Lin, S.-Y.; Tsai, T.-K.; Lin, C.-M.; Chen, C.-h.; Chan, Y.-C.; Chen, H.-W. *Langmuir* **2002**, *18*, 5473.
- (44) Cademartiri, L.; Mwangi, M. T.; Nijhuis, C. A.; Barber, J. R.; Sodhi, R. N. S.; Brodersen, P.; Kim, C.; Reus, W. F.; Whitesides, G. M. **2010**, unpublished.
- (45) Joachim, C. *New J. Chem.* **1991**, *15*, 223.
- (46) Manassen, Y.; Shachal, D. *Ann. N.Y. Acad. Sci.* **1998**, *852*, 277.
- (47) Shachal, D.; Manassen, Y. *Chem. Phys. Lett.* **1997**, *271*, 107.
- (48) Selzer, Y.; Salomon, A.; Cahen, D. *J. Phys. Chem. B* **2002**, *106*, 10432.
- (49) Sun, Q.; Selloni, A.; Scoles, G. *ChemPhysChem* **2005**, *6*, 1906.
- (50) Lindsay, S. M. *Jpn. J. Appl. Phys., Part 1* **2002**, *41*, 4867.
- (51) Wang, W.; Lee, T.; Reed, M. A. *Phys. Rev. B: Condens. Matter Mater. Phys.* **2003**, *68*, 035416/1.
- (52) Wang, W.; Lee, T.; Reed, M. A. *Nano Mol. Electron. Handb.* **2007**, *1*/1.
- (53) Slowinski, K.; Chamberlain, R. V.; Miller, C. J.; Majda, M. *J. Am. Chem. Soc.* **1997**, *119*, 11910.
- (54) Slowinski, K.; Fong, H. K. Y.; Majda, M. *J. Am. Chem. Soc.* **1999**, *121*, 7257.
- (55) Kim, Y.-H.; Jang, S. S.; Goddard, W. A., III *J. Chem. Phys.* **2005**, *122*, 244703/1.
- (56) Wang, G.; Yoo, H.; Na, S.-I.; Kim, T.-W.; Cho, B.; Kim, D.-Y.; Lee, T. *Thin Solid Films* **2009**, *518*, 824.
- (57) Song, H.; Kim, Y.; Ku, J.; Jang, Y. H.; Jeong, H.; Lee, T. *Appl. Phys. Lett.* **2009**, *94*, 103110/1.
- (58) Wang, G.; Kim, T.-W.; Jang, Y. H.; Lee, T. *J. Phys. Chem. C* **2008**, *112*, 13010.
- (59) Kim, T.-W.; Wang, G.; Lee, H.; Lee, T. *Nanotechnology* **2007**, *18*, 315204/1.
- (60) Lee, T.; Wang, G.; Klemic, J. F.; Zhang, J. J.; Su, J.; Reed, M. A. *J. Phys. Chem. B* **2004**, *108*, 8742.

- (61) Wang, W.; Lee, T.; Reed, M. A. *Physica E (Amsterdam, Neth.)* **2003**, *19*, 117.
- (62) Akkerman, H. B.; Blom, P. W. M.; de Leeuw, D. M.; de Boer, B. *Nature* **2006**, *441*, 69.
- (63) Akkerman, H. B.; de Boer, B. *J. Phys.: Condens. Matter* **2008**, *20*, 013001/1.
- (64) Akkerman, H. B.; Kronemeijer, A. J.; Harkema, J.; van Hal, P. A.; Smits, E. C. P.; de Leeuw, D. M.; Blom, P. W. M. *Org. Electron.* **2010**, *11*, 146.
- (65) Akkerman, H. B.; Kronemeijer, A. J.; van Hal, P. A.; de Leeuw, D. M.; Blom, P. W. M.; de Boer, B. *Small* **2008**, *4*, 100.
- (66) Akkerman, H. B.; Naber, R. C. G.; Jongbloed, B.; Van Halt, P. A.; Blom, P. W. M.; De Leeuw, D. M.; De Boer, B. *Proc. Natl. Acad. Sci. U.S.A.* **2007**, *104*, 11161.
- (67) Van Hal, P. A.; Smits, E. C. P.; Geuns, T. C. T.; Akkerman, H. B.; De Brito, B. C.; Perissinotto, S.; Lanzani, G.; Kronemeijer, A. J.; Geskin, V.; Cornil, J.; Blom, P. W. M.; De Boer, B.; De Leeuw, D. M. *Nature Nanotechnol.* **2008**, *3*, 749.
- (68) Strong, L.; Whitesides, G. M. *Langmuir* **1988**, *4*, 546.
- (69) Ulman, A. *Chem. Rev.* **1996**, *96*, 1533.
- (70) Chidsey, C. E. D.; Liu, G. Y.; Rowntree, P.; Scoles, G. *J. Chem. Phys.* **1989**, *91*, 4421.
- (71) Chidsey, C. E. D.; Loiacono, D. N. *Langmuir* **1990**, *6*, 682.
- (72) Outka, D. A.; Stohr, J.; Rabe, J. P.; Swalen, J. D.; Rotermund, H. H. *Phys. Rev. Lett.* **1987**, *59*, 1321.
- (73) Ulman, A.; Eilers, J. E.; Tillman, N. *Langmuir* **1989**, *5*, 1147.
- (74) Sellers, H.; Ulman, A.; Shnidman, Y.; Eilers, J. E. *J. Am. Chem. Soc.* **1993**, *115*, 9389.
- (75) Schlenoff, J. B.; Li, M.; Ly, H. *J. Am. Chem. Soc.* **1995**, *117*, 12528.
- (76) Weiss, E. A.; Kaufman, G. K.; Kriebel, J. K.; Li, Z.; Schalek, R.; Whitesides, G. M. *Langmuir* **2007**, *23*, 9686.
- (77) Weiss, E. A.; Chiechi, R. C.; Kaufman, G. K.; Kriebel, J. K.; Li, Z.; Duati, M.; Rampi, M. A.; Whitesides, G. M. *J. Am. Chem. Soc.* **2007**, *129*, 4336.
- (78) Song, H.; Lee, T.; Choi, N.-J.; Lee, H. *J. Vac. Sci. Technol., B: Microelectron. Nanometer Struct.—Process, Meas., Phenom.* **2008**, *26*, 904.
- (79) Song, H.; Lee, T.; Choi, N.-J.; Lee, H. *Appl. Phys. Lett.* **2007**, *91*, 253116/1.
- (80) He, J.; Forzani, E. S.; Nagahara, L. A.; Tao, N.; Lindsay, S. *J. Phys.: Condens. Matter* **2008**, *20*, 374120/1.
- (81) Cui, X. D.; Zarate, X.; Tomfohr, J.; Sankey, O. F.; Primak, A.; Moore, A. L.; Moore, T. A.; Gust, D.; Harris, G.; Lindsay, S. M. *Nanotechnology* **2002**, *13*, 5.
- (82) Cui, X. D.; Primak, A.; Zarate, X.; Tomfohr, J.; Sankey, O. F.; Moore, A. L.; Moore, T. A.; Gust, D.; Harris, G.; Lindsay, S. M. *Science* **2001**, *294*, 571.
- (83) Luo, L.; Frisbie, C. D. *J. Am. Chem. Soc.* **2010**, *132*, 8854.
- (84) Beebe, J. M.; Kim, B.; Gadzuk, J. W.; Frisbie, C. D.; Kushmerick, J. G. *Phys. Rev. Lett.* **2006**, *97*, 026801/1.
- (85) Kim, B.; Beebe, J. M.; Jun, Y.; Zhu, X. Y.; Frisbie, C. D. *J. Am. Chem. Soc.* **2006**, *128*, 4970.
- (86) Engelkes, V. B.; Frisbie, C. D. *J. Phys. Chem. B* **2006**, *110*, 10011.
- (87) Engelkes, V. B.; Beebe, J. M.; Frisbie, C. D. *J. Phys. Chem. B* **2005**, *109*, 16801.
- (88) Wold, D. J.; Frisbie, C. D. *J. Am. Chem. Soc.* **2001**, *123*, 5549.
- (89) Song, H.; Lee, H.; Lee, T. *Ultramicroscopy* **2008**, *108*, 1196.
- (90) Yoo, H.; Choi, J.; Wang, G.; Kim, T.-W.; Noh, J.; Lee, T. *J. Nanosci. Nanotechnol.* **2009**, *9*, 7012.
- (91) Kim, Y.; Song, H.; Kim, D.; Lee, T.; Jeong, H. *ACS Nano* **2010**, *4*, 4426.
- (92) Venkataraman, B.; Breen, J. J.; Flynn, G. W. *At. Force Microsc./Scanning Tunneling Microsc., [Proc. U.S. Army Natick Res., Dev. Eng. Cent. Symp.], 1st* **1994**, 117.
- (93) Venkataraman, B.; Breen, J. J.; Flynn, G. W. *J. Phys. Chem.* **1995**, *99*, 6608.
- (94) Venkataraman, B.; Flynn, G. W.; Wilbur, J. L.; Folkers, J. P.; Whitesides, G. M. *J. Phys. Chem.* **1995**, *99*, 8684.
- (95) Bumm, L. A.; Arnold, J. J.; Cygan, M. T.; Dunbar, T. D.; Burgin, T. P.; Jones, L., II; Allara, D. L.; Tour, J. M.; Weiss, P. S. *Science* **1996**, *271*, 1705.
- (96) Reed, M. A.; Zhou, C.; Muller, C. J.; Burgin, T. P.; Tour, J. M. *Science* **1997**, *278*, 252.
- (97) Chen, J.; Reed, M. A. *Chem. Phys.* **2002**, *281*, 127.
- (98) Lee, T.; Wang, W.; Reed, M. A. *Jpn. J. Appl. Phys., Part I* **2005**, *44*, 523.
- (99) Wang, W.; Lee, T.; Reed, M. A. *J. Phys. Chem. B* **2004**, *108*, 18398.
- (100) Kushmerick, J. G.; Holt, D. B.; Pollack, S. K.; Ratner, M. A.; Yang, J. C.; Schull, T. L.; Naciri, J.; Moore, M. H.; Shashidhar, R. *J. Am. Chem. Soc.* **2002**, *124*, 10654.
- (101) Kushmerick, J. G.; Holt, D. B.; Yang, J. C.; Naciri, J.; Moore, M. H.; Shashidhar, R. *Phys. Rev. Lett.* **2002**, *89*, 086802.
- (102) Kushmerick, J. G.; Naciri, J.; Yang, J. C.; Shashidhar, R. *Nano Lett.* **2003**, *3*, 897.
- (103) Ashwell, G. J.; Mohib, A.; Miller, J. R. *J. Mater. Chem.* **2005**, *15*, 1160.
- (104) Tran, E.; Rampi, M. A.; Whitesides, G. M. *Angew. Chem., Int. Ed.* **2004**, *43*, 3835.
- (105) York, R. L.; Slowinski, K. *J. Electroanal. Chem.* **2003**, *550–551*, 327.
- (106) Chabinyc, M. L.; Holmlin, R. E.; Haag, R.; Chen, X.; Ismagilov, R. F.; Rampi, M. A.; Whitesides, G. M. *ACS Symp. Ser.* **2003**, *844*, 16.
- (107) Anariba, F.; McCreery, R. L. *J. Phys. Chem. B* **2002**, *106*, 10355.
- (108) Slowinski, K.; Majda, M. *J. Electroanal. Chem.* **2000**, *491*, 139.
- (109) Slowinski, K.; Chamberlain, R. V., II; Bilewicz, R.; Majda, M. *J. Am. Chem. Soc.* **1996**, *118*, 4709.
- (110) Mann, B.; Kuhn, H. *J. Appl. Phys.* **1971**, *42*, 4398.
- (111) Bain, C. D.; Whitesides, G. M. *Angew. Chem., Int. Ed.* **1989**, *101*, 522.
- (112) Guo, Q.; Sun, X.; Palmer, R. E. *Phys. Rev. B: Condens. Matter Mater. Phys.* **2005**, *71*, 035406/1.
- (113) Heimel, G.; Romaner, L.; Zojer, E.; Bredas, J.-L. *Proc. SPIE* **2008**, *6999*, 699919/1.
- (114) Hostettler, M. J.; Murray, R. W. *Curr. Opin. Colloid Interface Sci.* **1997**, *2*, 42.
- (115) Kumar, A.; Abbott, N. L.; Biebuyck, H. A.; Kim, E.; Whitesides, G. M. *Acc. Chem. Res.* **1995**, *28*, 219.
- (116) Romaner, L.; Heimel, G.; Zojer, E. *Phys. Rev. B: Condens. Matter Mater. Phys.* **2008**, *77*, 045113/1.
- (117) Schreiber, F. *J. Phys.: Condens. Matter* **2004**, *16*, R881.
- (118) Ulman, A. *Thin Solid Films* **1996**, *273*, 48.
- (119) Ulman, A. *Mol. Solid State* **1999**, *2*, 1.
- (120) Ulman, A. *Acc. Chem. Res.* **2001**, *34*, 855.
- (121) Ulman, A.; Evans, S. D.; Shnidman, Y.; Sharma, R.; Eilers, J. E. *Adv. Colloid Interface Sci.* **1992**, *39*, 175.
- (122) Ulman, A.; Kang, J. F.; Shnidman, Y.; Liao, S.; Jordan, R.; Choi, G.-Y.; Zaccaro, J.; Myerson, A. S.; Rafailovich, M.; Sokolov, J.; Fleischer, C. *Rev. Mol. Biotechnol.* **2000**, *74*, 175.
- (123) Wang, W.; Lee, T.; Kretzschmar, I.; Routenberg, D.; Reed, M. A. *Tech. Dig.—Int. Electron Devices Meet.* **2004**, *531*.
- (124) Wang, W.; Lee, T.; Reed, M. A. *Rep. Prog. Phys.* **2005**, *68*, 523.
- (125) Wang, W.; Lee, T.; Reed, M. A. *Proc. IEEE* **2005**, *93*, 1815.
- (126) Wang, W.; Lee, T.; Reed, M. A. *Nanoscale Assembly* **2005**, *43*.
- (127) Wang, W.; Lee, T.; Reed, M. A. *Lect. Notes Phys.* **2005**, *680*, 275.
- (128) Whitesides, G. M.; Kriebel, J. K.; Love, J. C. *Sci. Prog.* **2005**, *88*, 17.
- (129) Whitesides, G. M.; Ferguson, G. S.; Allara, D.; Scherson, D.; Speaker, L.; Ulman, A. *Crit. Rev. Surf. Chem.* **1993**, *3*, 49.
- (130) Whitesides, G. M.; Gorman, C. B. In *The Handbook of Surface Imaging and Visualization*; Hubbard, A. T., Ed.; CRC Press Inc.: Boca Raton, FL, 1995; p 713.
- (131) Whitesides, G. M.; Laibinis, P. E. *Langmuir* **1990**, *6*, 87.
- (132) Salomon, A.; Cahen, D.; Lindsay, S.; Tomfohr, J.; Engelkes, V. B.; Frisbie, C. D. *Adv. Mater.* **2003**, *15*, 1881.
- (133) Milani, F.; Grave, C.; Ferri, V.; Samori, P.; Rampi, M. A. *ChemPhysChem* **2007**, *8*, 515.
- (134) Akkerman, H. B. Ph.D. Thesis, University of Groningen, 2008.

- (135) Ulman, A. *MRS Bull.* **1995**, *20*, 46.
- (136) Nijhuis, C. A.; Reus, W. F.; Whitesides, G. M. *J. Am. Chem. Soc.* **2009**, *131*, 17814.
- (137) Chiechi, R. C.; Weiss, E. A.; Dickey, M. D.; Whitesides, G. M. *Angew. Chem., Int. Ed.* **2008**, *47*, 142.
- (138) Nijhuis, C. A.; Reus, W. F.; Barber, J. R.; Dickey, M. D.; Whitesides, G. M. *Nano Lett.* **2010**, *10*, 3611.
- (139) Dickey, M. D.; Chiechi, R. C.; Larsen, R. J.; Weiss, E. A.; Weitz, D. A.; Whitesides George, M. *Adv. Funct. Mater.* **2008**, *18*, 1097.
- (140) Song, H.; Kim, Y.; Jeong, H.; Reed, M. A.; Lee, T. *J. Phys. Chem. C* **2010**, *114*, 20431.
- (141) Song, H.; Lee, H.; Lee, T. *J. Am. Chem. Soc.* **2007**, *129*, 3806.
- (142) Wang, G.; Kim, T.-W.; Jo, G.; Lee, T. *J. Am. Chem. Soc.* **2009**, *131*, 5980.
- (143) Reus, W. F.; Barber, J. R.; Thuo, M. M.; Nijhuis, C. A.; Whitesides, G. M., unpublished results.
- (144) Not to be confused with 95% prediction bands, which define the region in which the results of the next measurement are likely to appear.
- (145) It is also possible to perform linear regressions directly on  $\log(|J|)$  vs  $d$  without determining  $\mu_{\log}$  first. This direct approach offers distinct advantages but requires a more detailed analysis than we can present here; we will discuss this approach in a separate paper.
- (146) Holmlin, R. E.; Haag, R.; Chabiny, M. L.; Ismagilov, R. F.; Cohen, A. E.; Terfort, A.; Rampi, M. A.; Whitesides, G. M. *J. Am. Chem. Soc.* **2001**, *123*, 5075.
- (147) Holmlin, R. E.; Ismagilov, R. F.; Haag, R.; Mujica, V.; Ratner, M. A.; Rampi, M. A.; Whitesides, G. M. *Angew. Chem., Int. Ed.* **2001**, *40*, 2316.
- (148) Rampi, M. A.; Schueller, O. J. A.; Whitesides, G. M. *Appl. Phys. Lett.* **1998**, *72*, 1781.
- (149) Rampi, M. A.; Whitesides, G. M. *Chem. Phys.* **2002**, *281*, 373.